Geochemistry Geophysics Geosystems G3
AN ELECTRONIC JOURNAL OF THE EARTH SCIENCES
Published by AGU and the Geochemical Society

Article
Volume 4, Number 7
12 July 2003
1057, doi:10.1029/2002GC000451
ISSN: 1525-2027

Low-pressure phase equilibria of anhydrous anorthite-bearing mafic magmas

Edward J. Kohut
Department of Geosciences, Oregon State University, 104 Wilkinson Hall, Corvallis, Oregon 97331, USA (kohute@geo.orst.edu)

Roger L. Nielsen
Department of Geosciences and College of Oceanic and Atmospheric Sciences, Oregon State University, 104 Wilkinson Hall, Corvallis, Oregon 97331, USA

[1] One of the most persistent questions regarding the phase equilibria of mid-ocean ridge basalts (MORB) pertains to the petrogenesis of the anorthitic plagioclase phenocrysts (>An_{90}) that are characteristic of the more primitive members of such suites. Anorthitic phenocrysts are present in many if not most MORB suites in spite of the fact that no naturally occurring MORB glasses have ever been discovered to be in equilibrium with plagioclase more calcic than An_{85}. We have addressed this paradox by attempting to saturate natural basalts with anorthite in a series of 1 atm experiments using three different natural basaltic starting compositions: an N-MORB, an E-MORB, and a continental high-alumina basalt. To ensure duplication of the olivine and anorthite saturation observed in natural anorthite-bearing basalt, the experiments were run in $An_{93\text{-}6}$ capsules with Fo_{92} olivine added to the starting glass. The compositions of experimental liquids are generally colinear with the trends observed in the lava suites used as the source material for the starting glasses. Significantly, aluminous spinel (Al_2O_3 contents of 61–68 wt%) was produced at 1290°C in all compositions and chromites (Al_2O_3 contents of 33–42 wt%) at lower temperatures in N-MORB-derived liquids despite no spinel having been added to the starting mixture. In addition, the experiments produced basaltic liquid in equilibrium with both >Fo_{89} olivine and >An_{85} feldspar at temperatures of 1230° and 1210°. These liquids have compositions with Mg# (at% Mg/Mg + Fe^T*100) that range from 63 to >85. The TiO_2-MgO correlation indicates large (~16–23%) amounts of crystallization for each percent decrease in MgO. These results suggest the possibility that dry, anorthite-bearing basaltic magmas are the product of the interaction between primary melt and Al-spinel-bearing upper mantle. In addition, the results indicate that MORB magmas can undergo a large amount (>50%) of crystallization prior to reaching 8% MgO. Further, although anorthite-bearing magmas have characteristics consistent with their being a significant volumetric component of MORB "parent" magmas, the reaction mechanism suggested for their petrogenesis indicates that they are not necessarily primary magmas.

Components: 9812 words, 17 figures, 7 tables.

Keywords: anorthite; phase equilibria; MORB; Al-spinel; geochemistry; oceanic crust.

Index Terms: 3630 Mineralogy and Petrology: Experimental mineralogy and petrology; 3640 Mineralogy and Petrology: Igneous petrology; 3620 Mineralogy and Petrology: Crystal chemistry; 3035 Marine Geology and Geophysics: Midocean ridge processes; 3655 Mineralogy and Petrology: Major element composition.

Received 7 October 2002; **Revised** 18 February 2003; **Accepted** 3 April 2003; **Published** 12 July 2003.

Kohut, E. J., and R. L. Nielsen, Low-pressure phase equilibria of anhydrous anorthite-bearing mafic magmas, *Geochem. Geophys. Geosyst.*, *4*(7), 1057, doi:10.1029/2002GC000451, 2003.

1. Introduction

[2] Anorthitic feldspars are present in many mafic rocks, including arc lavas [*Marsh et al.*, 1990; *Sisson and Grove*, 1993; *Danyushevsky et al.*, 1997], ophiolite sequences [*Korenga and Kelemen*, 1997], and mid-ocean ridge basalts (MORB) [e.g., *Muir and Tilley*, 1964; *Ribbe*, 1983; *Natland*, 1989; *Allan et al.*, 1989; *Nielsen et al.*, 1995, and references within]. Despite their widespread occurrence, the petrogenesis of anhydrous anorthite-bearing basaltic magmas (MORB being the most common example) is not easily explained. It is generally accepted that the An content of feldspar can be increased either by increasing the H_2O content of the magma [*Sisson and Grove*, 1993] or by raising the Ca/Na or Al of the melt [*Fisk*, 1984; *Panjasawatwong et al.*, 1995]. Increasing pressure decreases the anorthite content of plagioclase at a rate of 1%An/kbar [*Fram and Longhi*, 1992], suggesting that anorthite phenocrysts in MORB have a shallow depth of origin. This depth has been placed as shallow as <3 kb by *Nielsen et al.* [1995], while *Maclennan et al.* [2001] report highAn feldspar that appeared to have formed at 8 kb pressure. While there are a few occurrences of anorthitic feldspar as quench phases in MORB glass [*Natland et al.*, 1983], high-An (>An_{88}) feldspars have never been produced experimentally from any naturally occurring MORB glass under dry conditions. Although synthetic anhydrous magmas have crystallized equilibrium high-An feldspars, the compositions of these melts do not resemble any naturally occurring basaltic lavas [*Panjasawatwong et al.*, 1995; *Nielsen et al.*, 1995].

[3] Most anorthitic feldspars in MORB are not in equilibrium with their host lava [*Dungan and Rhodes*, 1978; *Natland et al.*, 1983; *Sinton et al.*, 1993]. In terms of phase relations, the composition of melt inclusions hosted in MORB high-An crystals, together with the presence of spinel and olivine inclusions indicate that the natural anorthite phenocrysts crystallized in primitive (Mg# up to 75) melts that are three-phase saturated [*Nielsen et al.*, 1995; *Sours-Page et al.*, 2002]. Significantly, pyroxene is absent in these lavas. Knowledge of the phase equilibria of high-An feldspar is required in order to investigate the source and degree of melting responsible for the petrogenesis of anorthite-bearing MORBs. It is also needed to determine whether or not parent magmas of these MORBs are primary in the sense of being an unmodified product of partial melting, or have been modified by reaction with the upper mantle and crust before eruption.

[4] The petrogenesis of anorthite phenocrysts in MORB lavas has added significance in that they commonly contain large numbers of melt inclusions [*Sinton et al.*, 1993; *Nielsen et al.*, 1995]. In order to interpret the composition of melt trapped in anorthite, it is necessary to establish whether the anorthite phenocrysts are crystallization products of primary melting of a high-Ca/Na_2O (refractory) source, primary melting of a high-Al source, or products of reaction between primitive melts and the mantle or crust. If either of the first two cases is valid for anorthite formation, then the crystals may potentially trap primary melt. If the last case is valid, then the melt trapped by anorthite may be primitive and parental to more evolved lavas, but not technically primary.

[5] Some melt inclusion compositions suggest that high-An feldspar-bearing MORBs originate from refractory melts, i.e., those with low Na and Ti contents [*Natland*, 1989; *Johnson et al.*, 1995]. However, other examples of melt inclusion data from high-An feldspars in MORB are not simultaneously low in Na and Ti [*Nielsen et al.*, 1995; *Sours-Page et al.*, 1999, 2002]. In addition, *Sours-Page et al.* [2002] report that compositions of plagioclase-hosted melt inclusions from the East Pacific Rise are more evolved than inclusions in coexisting olivine phenocrysts. The compositions of the feldspar-hosted inclusions overlap those of the more primitive olivine-hosted inclusions and more evolved host lava, indicating that the feldspar

crystallized in a melt that was not primary, yet was parental to the erupted lava. Although many feldspar hosted melt-inclusions show compositional diversity that may be evidence for magma mixing between refractory and nonrefractory melts, the data of *Sours-Page et al.* [2002] reflect a more homogenous, nondepleted parent magma.

[6] In addition, derivation of data from anorthite hosted melt inclusions have several advantages over olivine hosted melt inclusions. First is the slow rate of diffusion of major elements compared to olivine [*Grove et al.*, 1984], which limits the potential modification by re-equilibration with the host magma, such as that observed in olivine-hosted inclusions [*Gaetani and Watson*, 2000]. The depth of entrapment is also constrained by the pressure limitations of anorthite formation noted above. In contrast, because basaltic magmas are saturated with respect to forsteritic olivine at all pressures [*Elthon*, 1989], we have no constraints on pressure from olivine hosted melt inclusions unless we obtain CO_2 measurements on the inclusions [*Cervantes and Wallace*, 2000]. Even in that case, we must assume that the pressure estimates based on CO_2 are maximum values. Anorthite hosted melt inclusions then provide a means of sampling melts assumed to be from depths <10 km. In any case, an understanding of the phase equilibria of high-An plagioclase-bearing melts is critical to interpretation of those melt inclusions.

[7] In this paper, we describe an experimental investigation of the question regarding the composition of basaltic liquids in equilibrium with high-An feldspar. This study is particularly relevant to the petrogenesis of those large, high-An (>85) feldspar phenocrysts present in many MORB lavas [*Sinton et al.*, 1993; *Nielsen et al.*, 1995; *Sours-Page et al.*, 1999]. Because it has been suggested that dry basaltic melts may be present in arcs [e.g., *Nye and Reid*, 1986; *Sisson and Bronto*, 1998], this study is also relevant to the petrogenesis of plagioclase-bearing arc basalts. We designed the experiments to produce an anhydrous, primitive (Mg# of 70–75) basaltic liquid that would crystallize $An_{>80}$ feldspars as an equilibrium phase. Ideally, one would start with naturally occurring glasses for this purpose, but basaltic glasses in equilibrium with high-An feldspar do not exist outside of melt inclusions. Instead, we chose to use natural basaltic glass and modify it by adding anorthitic components. This was achieved by melting the glass at high temperature while in contact within an anorthite capsule. The use of a feldspar capsule has several advantages over the typical procedure of doping glass with the desired component (in this case anorthite) and running in platinum crucibles. One is that the large crystal/melt ratio allows multiphase saturation without significantly affecting the average composition of feldspar that form as an equilibrium phase at run temperatures, and the capsule bulk reduces Na loss to furnace atmosphere. In addition, since the Pt suspension wire is in contact only with the capsule, Fe loss from the liquid is greatly reduced. We must emphasize that these experiments were not designed to model a natural process where basaltic magma reacts with plagioclase, nor should our results be interpreted in this context. The basaltic starting materials we used are not meant to represent a specific location or tectonic setting, but rather simulate three primitive basaltic magmas types of varying enrichment that are normally considered to be derived from dry decompression melting. These experiments used run temperatures ranging from 1200° to 1290°C.

2. Methods

2.1. Experimental Methods

[8] To fabricate experimental capsules, we used phenocrysts of $An_{93\text{-}6}$ plagioclase from Arenal Volcano, Costa Rica. The megacrysts were cut into ~5mm cubes and a hole ~2 mm in diameter and 3 mm deep was drilled into each capsule to hold the starting powder. The capsules were visually inspected to ensure that they did not have any glass from the feldspars' host lava. The starting powders consisted of ground glass from N-MORB, E-MORB, and continental high-alumina basalt (HAB). E-MORB starting materials were the least primitive, with Mg# averaging 59.98 and HAB materials were the most primitive (Table 1). HAB materials are also the lowest CaO/NaO_2 = 3.79 and were the most enriched, with a K_2O/TiO_2

Table 1. Compositions of Starting Glasses and Capsules[a]

	N-MORB		E-MORB		HAB			Arenal Feldspar	
Glasses	Avg	2σ	Avg	2σ	Avg	2σ	Capsule	Avg	2σ
				Starting Materials					
SiO_2	50.22	0.25	50.32	0.26	51.47	0.15	SiO_2	43.61	0.81
TiO_2	1.22	0.03	1.87	0.04	0.93	0.03	Al_2O_3	35.44	0.65
Al_2O_3	15.4	0.07	15.75	0.11	17.14	0.07	FeO*	0.44	0.05
Cr_2O_3	0.03	0.02	0.05	0.02	0.02	0.01	MgO	0.06	0.05
FeO*	9.28	0.06	9.21	0.09	7.26	0.36	CaO	19.32	0.47
MnO	0.15	0.03	0.16	0.03	0.15	0.03	Na_2O	0.47	0.19
MgO	8.54	0.05	7.43	0.05	7.88	0.17	K_2O	0.01	0.01
CaO	12.26	0.11	11.82	0.11	10.49	0.19	total	99.35	
Na_2O	2.19	0.04	2.73	0.04	2.77	0.06	n	61	
K_2O	0.05	0.01	0.59	0.01	0.75	0.02			
P_2O_5	0.11	0.03	0.27	0.02	0.16	0.02	An	95.75	1.663
total	99.45		100.2		99.02				
n	35		20		20				
Mg#	62.11		59.98	0.31	65.93	1.54			
CaO/Na_2O	5.6		4.53		3.79				
K_2O/TiO_2	0.04		0.32		0.81				

	Glass Analysis		Feldspar Analysis		Olivine Analysis		Spinel Analysis	
	± Error	2σ	± Error	2σ	± Error	2σ	± Error	2σ
				EMP Accuracy and Precision				
SiO_2	0.8%	0.08	0.6%	0.20	1.3%	0.07		
TiO_2	3.1%	0.04						
Al_2O_3	1.0%	0.07	0.5%	0.04			0.6%	0.02
FeO*	12.9%	0.12			0.2%	0.10	5.0%	0.13
MgO	2.3%	0.04			0.9	0.07	7.0%	0.04
CaO	1.1%	0.08	1.5%	0.05				
Na_2O	2.7%	0.04	2.6%					
Cr_2O_3	-		-				1.1%	0.08

[a] Maximum error reported for significant elements of each analyses routine. ± error calculated for each analysis routine by [(measured)-true/measured]*100. Precision reported as 2σ.

ratio of 0.81 (Table 1). N-MORB starting glass were the least enriched and most refractory (K_2O/TiO_2 = 0.04, CaO/NaO_2 = 5.6; Table 1). However, it must be noted that these were the compositions of the glasses before being saturated in anorthite.

[9] The N-MORB was sampled from Gorda Ridge lava (D9-2 [*Davis and Clague*, 1987]), the E-MORB from the Endeavour segment of the Juan de Fuca Ridge (E-32 [*Karsten et al.*, 1990]), and the high-alumina basalt from Medicine Lake in California (Giant Crater [*Baker et al.*, 1991; *Donnelly-Nolan et al.*, 1991]). Kilbourne Hole olivine (Fo_{91-92}) was added to ensure olivine saturation. The rationale behind using whole olivine crystals is the same as that for using anorthite capsules, i.e., the bulk ensures allows multiphase saturation without significantly affecting the average composition of the olivine that form at equilibration run temperatures. In addition, 0.1 wt% ZrO_2 was added to distinguish the products of our experiments from any small amount of glass that may have escaped visual inspection of the capsule material. This was done in the event that any of our experimental glass flowed into cracks in the capsules, which had occurred in earlier experiments using feldspar capsules from a different source. In such circumstances, it would be necessary to distinguish, via the ZrO_2 dopant, the experimental glass from any natural glass in the cracks. However, with Arenal feldspar

capsules the experimental liquids remained confined to the hole drilled into the capsule.

[10] The charges were suspended by platinum wire in a Deltec vertical quench furnace and the oxygen fugacity was set at the QFM buffer using a mixture of CO_2 and H_2. An initial run temperature of 1300°C for two hours was used to saturate the melt in anorthite and olivine, this temperature will be referred to as the initial melting temperature. Re-homogenization experiments of plagioclase-hosted melt inclusions [*Johnson et al.*, 1995; *Sinton et al.*, 1993; *Nielsen et al.*, 1995; *Sours-Page et al.*, 1999] show that most entrapment temperatures in MORB are below 1260°–1280°. Since this suggests that many high-An feldspar in MORB were crystallize at or below these temperatures, we selected 1300° as the point at which we saturate the melt in anorthitic components (i.e., raise the Al and Ca/Na levels). One experiment for each starting material was held at the melting temperature for 6 hours, then quenched. The purpose for this experiment was to observe the composition of the saturated melt prior to being lowered to the equilibration temperatures. Otherwise, after the initial heating to 1300°C, the experimental charge was dropped to run temperature for 24 hours; we will refer to this temperature as the equilibration temperature. At the end of the run time, the charges were drop-quenched in water.

[11] The first set of experiments was done using only N-MORB glass (no forsterite) in anorthite capsules to provide baseline data melts saturated with feldspar only. This is similar to the approach used by *Panjasawatwong et al.* [1995]. The second set of experiments added whole forsterite crystals to the glass and ran at equilibration temperatures of 1290°, 1260°, 1230°, and 1210° C. A single experiment run for two hours at 1300° showed no significant difference compared to the 6-hour run. The experiments in second set successfully produced mafic liquids that crystallized anorthite and forsterite at 1230°, and 1210° C. We then repeated these experiments using E-MORB and HAB starting powders.

[12] To test the effects of changing the initial melting temperature and the degree of undercooling (ΔT = initial T-equilibration T), we conducted a third set of experiments. In these, the run temperature was fixed at 1210° C, which was found from the results of the second experimental set to be favorable for high-An feldspar crystallization. Initial melting temperatures of 1280°, 1250°, and 1220° C were used to reproduce the same amounts of undercooling as those in the second set of experiments. These experiments were run using only the N-MORB starting glass.

2.2. Analytical Methods

[13] Run products were analyzed with the Cameca SX-50 electron microprobe at Oregon State University using a 15 kV, 30nA, 3 micron diameter beam for glass and feldspar, and 15 kV, 50 nA, 1 micron diameter beam for olivine. For glass, count times were 30s for Fe, 20s for Mg, Al, Si, P, K, Ti and Zr, and 10s for Na, Ca, Cr, and Mn. For feldspar, count times were 10 seconds for all elements. For olivine, count times were 20s for Fe, Si, and Ni, and 10s for Mg, Al, Si, K, Ti, Na, Ca, Cr, and Mn. To minimize the effects of Na migration, Na was analyzed first. Precision and accuracy measurements for the most significant elements in the glass, feldspar, olivine and spinel analyses routines are listed in Table 1.

3. Results

3.1. Experiment Set 1: Anorthite Saturated Melt

[14] The first experiments using N-MORB glass saturated with anorthite only (without added forsterite) produced $An_{76.9-79.7}$ feldspar at temperatures 1230° and 1200°. Feldspar only crystallized at temperatures below 1250° and feldspar compositions were never higher than $An_{79.7}$, although the composition of the reaction zone on the capsule rim was $An_{84.3}$ at 1250° equilibration temperature and $An_{92.7}$ at the 1300° melting temperature (Table 2, Figure 1). Predicted values for An content were calculated using equation (1) of *Panjasawatwong et al.* [1995] and the Ca# and An# of our experimental melts. Except for the 1230° run, neither the An content of the experimentally produced feldspars nor the reaction zones on the capsules were similar to the predicted values. While the An

Table 2. Summary of Experimental Results[a]

Equilibration Temp, °C	Glass Mg#	Glass Ca#	Glass Al#	Capsule Rim An	Feldspar An			
Experiment Set 1: Anorthite Saturated, N-MORB Starting Material, 1300°C Melting Temperature								
1200	67.5	49.1	28.8	84.3	77.6			
1230	65.6	75.8	26.9	87.7	79.7			
1250	67.5	68.1	28.1	84.3	none			
1300	67.1	70.4	31.0	92.7	none			
Temp, °C	Glass Mg#	Glass Ca#	Glass Al#	Capsule Rim An	Feldspar An	Added Ol Rim Fo	Olivine Fo	Spinel Cr#
Experiment Set 2: Anorthite and Forsterite Saturated, N-MORB Starting Material, 1300°C Melting Temperature								
1210	69.4	81.8	27.0	85.4	84.1	none	89.0	0.34
1230	69.7	84.2	27.8	88.2	87.0	none	90.2	0.38
1260	76.9	89.8	29.9	92.7	none	none	92.2	0.31
1290	82.0	88.3	33.7	95.4	none	92.2	none	0.03
1290[b]	82.2	89.9	34.5	95.3	none	91.7	none	0.05
1300	83.4	94.1	31.7	95.2	none	90.9	none	none
Equilibration Temp, °C	Glass Mg#	Glass Ca#	Glass Al#	Capsule Rim An	Feldspar An	Added Ol Rim Fo	Olivine Fo	Spinel Cr#
E-MORB Starting Material, 1300°C Melting Temperature								
1210	63.2	81.3	27.2	87.2	86.1	none	86.7	none
1230	67.3	82.0	29.0	87.2	86.6	none	89.4	none
1260	81.3	83.7	31.7	92.3	none	none	93.7	none
1290	83.5	87.0	34.0	95.4	none	91.0	none	0.01
1300	85.4	87.7	30.8	95.1	none	none	none	none
Equilibration Temp, °C	Glass Mg#	Glass Ca#	Glass Al#	Capsule Rim An	Feldspar An	Added Ol Rim Fo	Olivine Fo	Spinel Cr#
HAB Starting Material, 1300°C Melting Temperature								
1210	63.2	81.2	27.2	84.9	81.5	none	86.9	none
1230	65.9	86.0	28.9	87.6	85.6	none	88.8	0.01
1260	76.2	82.6	32.1	90.4	none	none	none	none
1290	79.0	82.7	33.5	94.8	none	91.4	none	0.01
1300	84.4	90.8	35.3	95.6	none	none	none	none
Melting Temp, °C	Glass Mg#	Glass Ca#	Glass Al#	Capsule Rim An	Feldspar An	Added Ol Rim Fo	Olivine Fo	Spinel Cr#
Experiment Set 3: Variable Melting Temperatures, N-MORB Starting Material, 1210°C Equilibration Temperature								
1220	66.9	82.2	25.8	95.6	95.5	none	87.8	0.37
1250	67.4	83.8	25.5	92.3	92.8	none	88.7	0.38
1280	69.4	84.3	25.9	88.3	88.5	none	88.9	0.38

[a] Feldspar An-feldspar crystallized in glass, Capsule rim An-An of reaction rim of capsule adjacent to melt, Olivine Fo, Fo of olivine in melt, Added Olivine Fo, Fo of rim of remnant added olivine. Mg# = at% Mg/(Mg+Fe^T)*100, Ca# = at% Ca/(Ca+Na)*100, Al# = at% Al/(Al+Si)*100.
[b] Four hour equilibration time.

content of the feldspars and the MgO of the host liquid at 1200° and 1230° were similar to An content of some feldspars and their host glass reported by *Natland* [1989, Tables 1 and 5], the Al contents of the experimental liquids were higher. The liquids had Mg# (atomic% Mg/Mg + Fe_T*100) of 62.4–67.5, 1.7–2.31 wt% Na_2O and 15.43–19.73 wt% Al_2O_3 (Figure 2, Tables 2 and 3). No examples of MORB glass in the precompiled RIDGE petrologic database (available at http://petdb.ldeo.columbia.edu/readydata/MAR55S-52N_major_probe.csv) (hereinafter referred to as RIDGE PETDB) had Al_2O_3 as high as the glasses for these experiments and TiO_2 contents were lower than any glass in the database with MgO contents similar to the experimental liquids (Table 2, Figure 2). The glass compositions were similar to some of the refractory melt inclusions reported by *Johnson et al.* [1995],

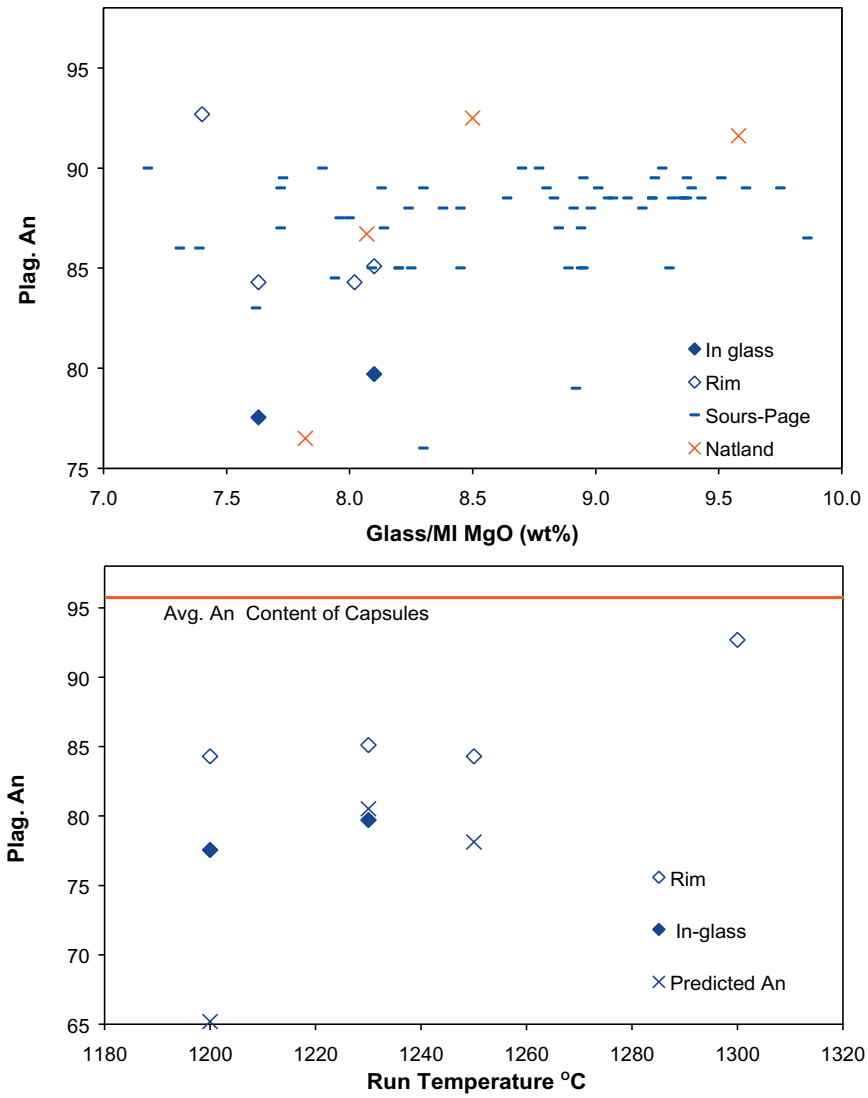

Figure 1. (top) An content of feldspars from experiment set 1 versus MgO of host liquid. "Sours-Page" refers to host feldspar An and melt inclusion MgO from *Sours-Page et al.* [1999, 2002] and "Natland" refers to feldspar An and host glass MgO from *Natland* [1989]. "Rim" refers to capsule rim reaction zone, "In-glass" are feldspars that crystallized from the melt. (bottom) An content of feldspars and capsule reaction zones from experiment set 1 versus equilibration temperatures. "Predicted" are the An values of feldspar predicted for the melt composition.

but the host feldspars in reported in that paper had higher An contents than our experimental feldspars. The major element contents of liquids for these experiments were similar to those of the *Panjasawatwong et al.* [1995] that produced plagioclase only, except that our glasses had higher Mg# and ~1–3 wt% higher MgO contents.

3.2. Experiment Set 2: Anorthite and Forsterite Saturated Melt

[15] In the second set of experiments, we added whole olivine crystals to drive the melt to saturation with forsterite as well as anorthite components at high temperature (>1260°). As a result, the lower temperature experiments had melts that nucleated both feldspar and olivine. In addition, Al-rich spinel was present in the 1290° runs in this set of experiments, indicating that at higher temperatures the melt was in equilibrium with this third phase.

[16] The Mg# of liquids decreased from 83.4 at 1300° to 69.4 at 1210° for N-MORB, from 85.4 to 63.2 for E-MORB, and 84.4 to 63.2 for HAB starting compositions (Table 2). At 1260°, the Mg# of glasses approximate those of hypothetical

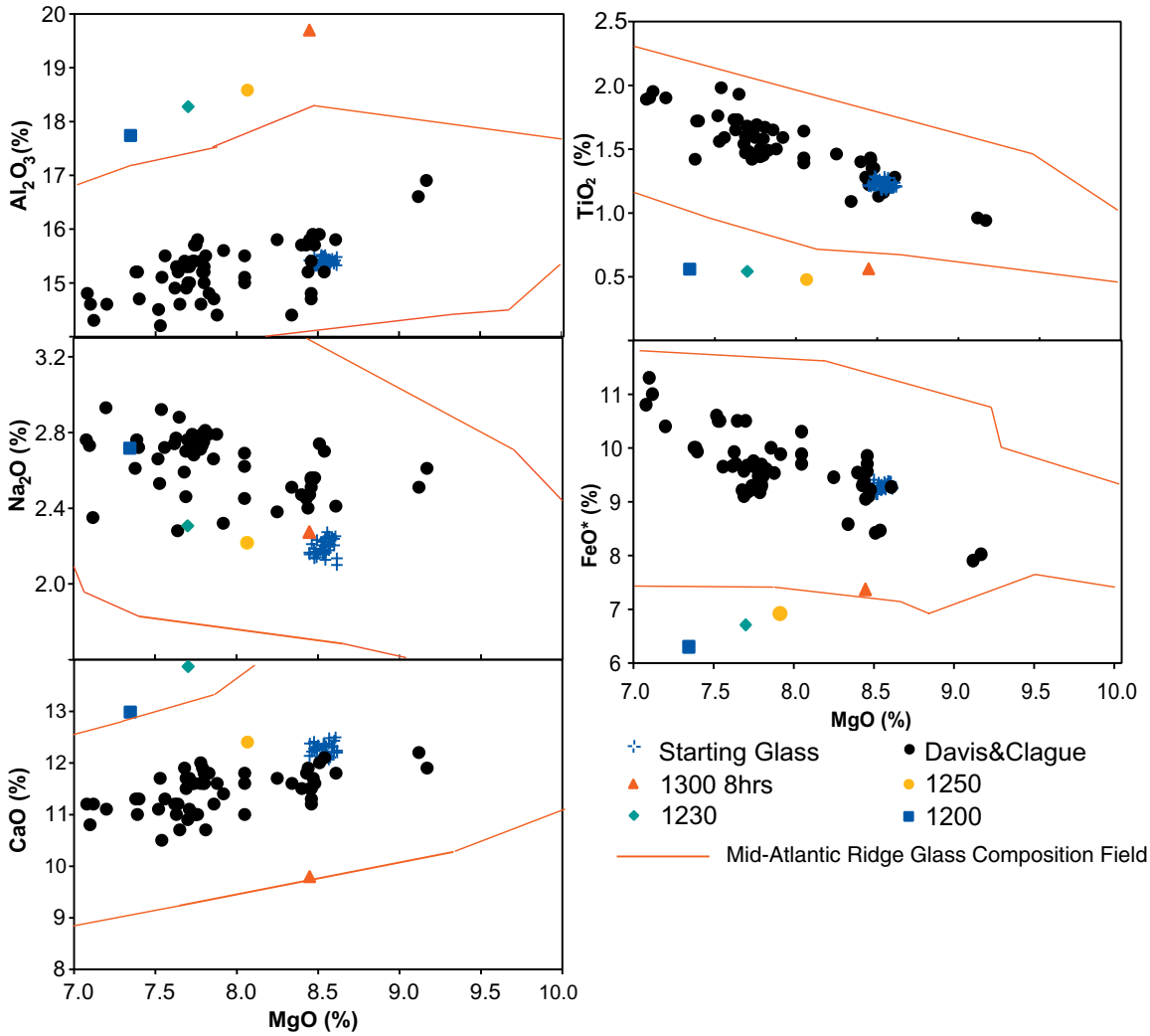

Figure 2. Al_2O_3, Na_2O, CaO, TiO_2 and FeO* versus MgO of glasses for experiment set 1. Numbers refer to equilibration temperatures. Run times were 18 hrs except where noted. "Davis and Clague" refers to compositions from the Gorda Ridge from *Davis and Clague* [1987]. Region outlined in red contains range of Mid-Atlantic Ridge glass compositions in the pre-compiled RIDGE petrologic database (RIDGE PETDB).

MORB parent magmas (assumed to be in equilibrium with mantle olivine), which range from 70 to 77 [*Basaltic Volcanism Study Project* (*BVSP*), 1981]. At 1260°, the N-MORB-derived liquids Mg# averaged 76.9, E-MORB-derived Mg# were 81.3, and HAB-derived Mg# were 76.2 (Table 2), and the melts were in equilibrium with high-Fo olivine, as indicated by the presence of this phase in the run products. The glass compositions at 1230° were similar to natural, primitive basalts: the N-MORB-, E-MORB-, and HAB-derived melts have average Mg# of 69.7, 67.3, and 65.9 respectively (Table 2). Furthermore, the presence of high-An feldspar and high-Fo olivine indicates that the melts were in equilibrium with these phases at this temperature.

[17] At all temperatures, the rims of the anorthite capsules adjacent to the liquids contained a reaction zone and the An content of these reaction rims decreased with run temperature (Figure 3). A reaction rim of ~10 μm was present at the capsule/glass interface for N-MORB and HAB starting materials at 1300°. This rim was $An_{92.6}$ for N-MORB and $An_{94.8}$ for HAB, while the rim in the E-MORB experiments was unchanged from the

Table 3. Glass Compositions for Experiments

	1300° Melt T		1250° Equil. T		1230° Equil. T		1200° Equil. T.	
	Avg	2σ	Avg	2σ	Avg	2σ	Avg	2σ
Experiment Set 1: Anorthite Saturated								
N-MORB starting material, 1300°C melting temp.								
SiO_2	51.77	0.11	50.65	0.44	50.10	0.55	51.71	0.03
TiO_2	0.56	0.03	0.48	0.02	0.54	0.05	0.56	0.05
Al_2O_3	19.7	0.12	18.58	0.10	18.28	0.09	17.74	0.09
Cr_2O_3	0.02	0.02	0.01	0.02	0.03	0.02	0.03	0.02
FeO*	7.37	0.02	6.91	0.09	6.71	0.20	6.30	0.04
MnO	0.19	0.05	0.20	0.03	0.20	0.02	0.08	0.04
MgO	8.45	0.07	8.07	0.07	7.70	0.19	7.35	0.05
CaO	9.8	0.09	12.40	0.48	13.87	0.33	12.98	0.13
Na_2O	2.27	0.05	2.22	0.03	2.31	0.10	2.72	0.03
K_2O	0.07	0.01	0.09	0.01	0.06	0.04	0.07	0.04
P_2O_5	0.09	0.02	0.07	0.01	0.08	0.04	0.08	0.02
total	100.29		99.68		99.88		99.62	
n	10		10		5		10	
Ca/Na	4.32		5.59		6.00		4.77	
K/Ti	0.13		0.19		0.11		0.13	

	1300° Equil. T.		1290° Equil. T.		1290° Equil. T.[a]		1260° Equil. T.		1230° Equil. T.		1210° Equil. T.	
	Avg	2σ	Avg	2σ	Avg	2σ	Avg	2σ	Avg	2σ	Avg	2σ
Experiment Set 2: Anorthite and Forsterite Saturated												
N-MORB Starting material, 1300° C melting temp.												
SiO_2	46.83	0.12	46.79	0.20	47	0.28	48.97	0.12	49.32	0.15	50.91	0.14
TiO_2	0.38	0.01	0.46	0.01	0.41	0.06	0.75	0.01	0.94	0.03	1.09	0.02
Al_2O_3	20.91	0.24	20.16	0.20	20.55	0.65	17.75	0.09	16.18	0.08	15.00	0.25
Cr_2O_3	0.03	0.02	0.02	0.02	0.03	0.02	0.07	0.02	0.08	0.02	0.11	0.04
FeO*	4.77	0.04	5.45	0.10	5.16	0.08	6.41	0.08	7.92	0.10	7.98	0.02
MnO	0.09	0.02	0.09	0.03	0.09	0.02	0.15	0.02	0.16	0.03	0.17	0.04
MgO	13.41	0.29	13.25	0.22	13.21	0.48	11.92	0.07	10.24	0.08	9.76	0.06
CaO	13.76	0.13	13.93	0.31	13.82	0.24	13.87	0.11	14.09	0.22	14.02	0.21
Na_2O	0.85	0.02	0.88	0.04	0.99	0.04	0.88	0.04	1.42	0.05	1.40	0.04
K_2O	0.02	0.01	0.05	0.01	0.03	0.01	0.07	0.01	0.08	0.01	0.08	0.01
P_2O_5	0.04	0.02	0.08	0.02	0.04	0.02	0.09	0.03	0.09	0.03	0.11	0.02
total	101.09		101.06		101.33		100.93		100.52		100.63	
n	5		15		31		16		22		8	
Ca/Na	16.19		15.83		13.96		15.76		9.92		10.01	
K/Ti	0.05		0.11		0.07		0.09		0.09		0.07	
E-MORB Starting material, 1300° C melting temp.												
SiO_2	46.56	0.18	47.31	0.18			48.11	0.43	48.11	0.39	48.69	0.35
TiO_2	0.73	0.05	0.80	0.02			1.14	0.03	1.62	0.03	1.90	0.05
Al_2O_3	20.64	0.37	20.71	0.16			18.94	0.10	16.67	0.06	15.41	0.11
Cr_2O_3	0.02	0.03	0.02	0.03			0.02	0.02	0.03	0.02	0.03	0.03
FeO*	4.55	0.20	4.72	0.08			4.79	0.06	8.43	0.05	9.24	0.10
MnO	0.11	0.03	0.11	0.01			0.12	0.03	0.15	0.03	0.17	0.03
MgO	13.58	0.22	13.02	0.07			11.7	0.09	9.72	0.08	8.89	0.10
CaO	13.2	0.14	12.76	0.09			12.15	0.12	12.39	0.08	12.94	0.36
Na_2O	0.98	0.05	1.06	0.05			1.30	0.04	1.50	0.05	1.64	0.04
K_2O	0.25	0.01	0.21	0.01			0.31	0.01	0.45	0.01	0.47	0.02
P_2O_5	0.18	0.03	0.08	0.01			0.15	0.02	0.22	0.03	0.25	0.03
total	100.8		100.8				98.73		99.29		99.63	
n	15		16				21		12		13	
Ca/Na	1.347		12.04				9.35		8.26		7.89	
K/Ti	0.34		0.26				0.27		0.28		0.25	

Table 3. (continued)

	1300° Equil. T.		1290° Equil. T.		1290° Equil. T.[a]		1260° Equil. T.		1230° Equil. T.		1210° Equil. T.	
	Avg	2σ	Avg	2σ	Avg	2σ	Avg	2σ	Avg	2σ	Avg	2σ
HAB starting material, 1300° C melting temp.												
SiO_2	46.44	0.53	48.17	0.31			48.25	0.38	50.11	0.05	52.36	0.23
TiO_2	0.28	0.02	0.5	0.03			0.063	0.02	0.97	0.02	1.21	0.02
Al_2O_3	21.65	0.15	20.75	0.11			19.37	0.10	17.29	0.10	16.05	0.07
Cr_2O_3	0.01	0.02	0.03	0.03			0.03	0.02	0.03	0.02	0.02	0.01
FeO*	4.39	0.10	5.73	0.10			6.34	0.09	8.58	0.11	7.56	0.04
MnO	0.08	0.02	0.11	0.03			0.11	0.02	0.13	0.02	0.16	0.04
MgO	13.34	0.17	12.1	0.09			11.35	0.09	9.31	0.05	8.00	0.06
CaO	13.29	0.12	11.87	0.12			11.62	0.08	11.1	0.08	11.3	0.03
Na_2O	0.76	0.03	1.34	0.04			1.33	0.04	1.53	0.04	1.91	0.03
K_2O	0.15	0.01	0.35	0.02			0.36	0.01	0.58	0.02	0.80	0.01
P_2O_5	0.05	0.02	0.08	0.02			0.08	0.02	0.125	0.01	0.15	0.03
total	100.44		101.03				99.47		99.75		99.52	
n	18		19				14		6		13	
Ca/Na	17.49		8.86				8.74		7.25		5.92	
K/Ti	0.54	0.70					0.57		0.60		0.66	

	1280° Melt T.		1250° Melt T.		1220° Melt T.	
	Avg	2σ	Avg	2σ	Avg	2σ
Experiment Set 3: Anorthite and Forsterite Saturated Variable Melting Ts						
N-MORB starting material, 1210° C equilibration temp.						
SiO_2	50.13	0.71	50.87	0.58	51.07	0.73
TiO_2	1.19	0.11	1.13	0.03	1.13	0.04
Al_2O_3	14.87	0.53	14.73	0.24	14.98	0.08
Cr_2O_3	0.08	0.04	0.09	0.04	0.10	0.03
FeO*	7.66	0.53	8.13	0.12	7.90	0.59
MnO	0.14	0.03	0.13	0.03	0.13	0.02
MgO	9.77	0.77	9.44	0.16	9.38	0.11
CaO	14.75	0.53	14.3	0.22	14.14	0.14
Na_2O	1.52	0.05	1.53	0.05	1.68	0.05
K_2O	0.07	0.01	0.06	0.01	0.06	0.01
P_2O_5	0.11	0.03	0.11	0.02	0.11	0.02
total	100.29		100.52		100.68	
n	14		16		17	
Ca/Na	9.70		9.35		8.42	
K/Ti	0.06		0.05		0.05	

[a] Experiment with 4 hour run time.

starting capsule composition (Table 2). At temperatures of 1230° and below the reaction zone included new overgrowth. This was also the highest temperature at which plagioclase nucleated in the liquid. The An value of the reaction rims and liquid MgO at 1260° were similar to host feldspar An and melt inclusion MgO reported by *Sours-Page et al.* [1999, 2002], and somewhat similar to those of inclusions and feldspars in *Natland* [1989] (Figure 3). At 1230°, N-MORB-derived liquids crystallized An_{87} feldspar, E-MORB liquids produced $An_{86.6}$ feldspar, while HAB-derived liquids produced $An_{85.6}$ feldspar (Tables 2 and 4, Figure 3). The An contents of the feldspars at low temperatures and the reaction rims at higher temperatures were generally in good agreement with the values predicted using *Panjasawatwong et al.* [1995, equation (1)] (Figure 3). The An contents of the feldspars at 1230° and 1210° and the MgO values of the liquids they formed in were also similar to those of feldspars and their melt inclusions reported by *Sours-Page et al.* [1999, 2002].

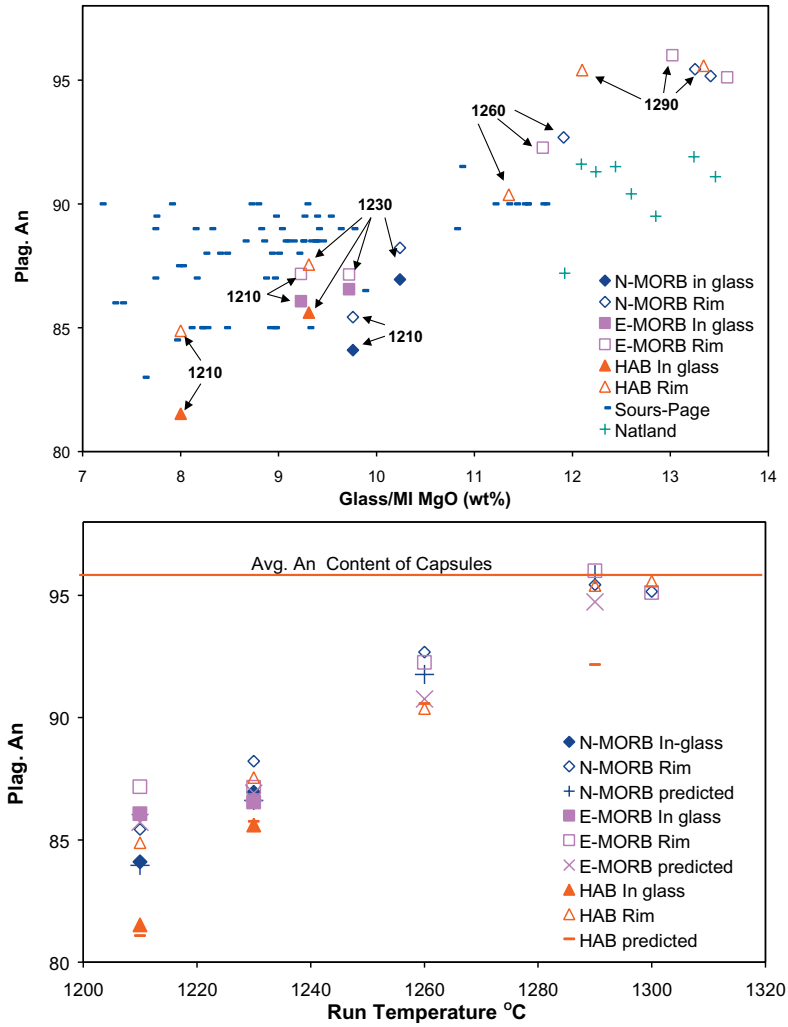

Figure 3. (top) An content of feldspars from Experiment Set 2 versus MgO of host liquid. "Sours-Page" refers to host feldspar An and melt inclusion MgO from *Sours-Page et al.* [1999, 2002] and "Natland" refers to host feldspar An and MI MgO from *Natland* [1989]. "Rim" refers to capsule rim reaction zone, "In-glass" are feldspars that crystallized from the melt. (bottom) An content of feldspars and capsule reaction zones from Experiment Set 2 versus equilibration temperatures. "Predicted" are the An values of feldspar predicted for the melt composition.

[18] New olivine nucleated in liquids from all starting compositions at temperatures of 1260° C and below. Remnants of the Kilbourne Hole forsterite added to the starting glass were present in all 1290° melts of experiment set 2, and at 1210° as well for the HAB composition. The compositions of olivines that crystallized in the liquids were consistently greater than Fo_{86} (Tables 2 and 5). The olivines produced at 1230° in N-MORB-, E-MORB-, and HAB-derived melts were $Fo_{90.2}$, $Fo_{89.4}$, and $Fo_{88.8}$ respectively. Equilibrium FeO/MgO ratios of olivines were predicted using *Roeder and Emslie*'s [1970] FeO/MgO melt-solid partitioning coefficient of 0.3. Overall, the FeO/MgO ratios of olivines produced during experiments with E-MORB-derived liquids were closer to the values predicted than those in N-MORB- and HAB-derived liquids (Figure 4). At 1230°, olivines in both the N-MORB- and HAB-derived melts were further from equilibrium compared to the 1210° experiments.

[19] In experiments run at 1290°, Al-spinel crystallized in the liquid adjacent to the capsule wall (Figure 5). At this temperature, the spinels in the N-MORB liquids had Al_2O_3 contents of 57-67.8 wt% and Cr# (Cr/Cr+Al) of 0.02–0.11 (Table 6). Those in the E-MORB liquids had an average

Table 4. Compositions of Feldspars Formed in Melt

	1230° Equil. T.					
	Avg	2σ				
Experiment Set 1: Anorthite Saturated						
N-MORB starting material, 1300°C melting temp						
SiO_2	48.69	0.00				
Al_2O_3	32.03	0.01				
FeO*	0.50	0.00				
MgO	0.23	0.02				
K_2O	0.06	0.01				
CaO	15.63	0.07				
Na_2O	2.21	0.02				
Total	99.34					
n	3					
An	79.74	0.19				
	1230° Equil. T.		1210° Equil. T.			
	Avg	2σ	Avg	2σ		
Experiment Set 2: Anorthite and Forsterite Saturated						
N-MORB starting material						
SiO_2	46.81	0.42	48.12	0.55		
Al_2O_3	33.82	0.22	32.99	0.39		
FeO*	0.45	0.08	0.44	0.00		
MgO	0.35	0.03	0.44	0.05		
K_2O	0.01	0.01	0.06	0.01		
CaO	17.78	0.17	16.4	0.13		
Na_2O	1.47	0.07	1.72	0.23		
Total	99.22		98.45			
n	12		5			
An	86.95	0.59	84.05	1.91		
E-MORB starting material						
SiO_2	46.49	0.30	45.54	0.35		
Al_2O_3	33.34	0.42	32.81	0.87		
FeO*	0.48	0.20	0.61	0.35		
MgO	0.38	0.25	0.48	0.32		
K_2O	0.08	0.02	0.08	0.02		
CaO	17.28	0.13	17.03	0.35		
Na_2O	1.48	0.09	1.52	0.15		
Total	98.05		96.55			
n	10		10			
An	86.55	0.80	86.07	1.45		
HAB starting material						
SiO_2	47.16	0.47	47.68	0.50		
Al_2O_3	33.47	0.47	32.36	0.27		
FeO*	0.50	0.11	0.54	0.08		
MgO	0.34	0.15	0.40	0.04		
K_2O	0.09	0.02	0.13	0.02		
CaO	17.39	0.37	16.19	0.25		
Na_2O	1.62	0.18	2.03	0.13		
Total	98.95		97.3			
n	7		8			
An	85.61	1.59	81.53	1.12		

Table 4. (continued)

	1280°Melt T.		1250° Melt T.		1220° Melt T.	
	Avg	2σ	Avg	2σ	Avg	2σ
Experiment Set 3: Anorthite and Forsterite Saturated Variable Melting Temperatures						
N-MORB starting material, 1210°C equilibration temp.						
SiO_2	46.25	1.77	42.35	2.92	43.53	0.41
Al_2O_3	33.51	1.59	36.14	2.54	35.33	0.40
FeO*	0.52	0.16	1.124	0.06	0.48	0.06
MgO	0.35	0.24	0.05	0.03	0.09	0.12
K_2O	0.01	0.01	0.00	0.01	0.01	0.01
CaO	18.05	1.19	19.21	1.12	19.3	0.23
Na_2O	1.29	0.63	0.93	0.07	0.5	0.10
Total	98.69		98.87		98.74	
n	28		17		23	
An	88.51	5.62	92.88	0.93	95.55	0.86

Al_2O_3 content of 68.35 wt% and Cr# of 0.01 and those in HAB liquids had an average Al_2O_3 content of 67.21 wt% and Cr# of 0.01 (Table 6). The formations of Al-spinels in bands suggests the presence of a compositional gradient in the melt, but none was observed in EMP traverses across the glass, even in the experiment with a 4-hour equilibration period. This indicates that any gradients or melt diversity had dissipated within four hours equilibration time. At the lower equilibration temperatures (1210°, 1230° and 1260°), the N-MORB-derived liquids produced chromite (Cr# of 0.31–0.38) with Al_2O_3 contents of 32.95–41.51 wt% (Table 6), but this phase was not present in the E-MORB- and HAB-derived melts. At 1230°, the HAB-derived melt produced Al-spinel (Al_2O_3 of 67.97 wt% and Cr# of 0.01) within the An_{86} feldspar overgrowth on the rim of the capsule; this was the only occurrence of aluminous spinel noted at lower temperatures (<1260°C).

[20] The compositions of our lower temperature spinels from N-MORB experiments were colinear with chromite compositions reported by *Allan et al.* [1989] for the Lamont seamounts (Figure 6). The spinels at 1260° were comparable in Cr# and Al content to the most Cr-rich spinels in abyssal peridotites [*Dick and Bullen*, 1984; *Dick*, 1989], spinel in lherzolite xenoliths [*BVSP*, 1981] and

Table 5. Compositions of Olivines Formed in Melt

	1260° Equil. T.		1230° Equil. T.		1210° Equil. T.	
	Avg	2σ	Avg	2σ	Avg	2σ
Experiment Set 2: Anorthite and Forsterite Saturated						
N-MORB starting material, 1300°C melting temp.						
SiO_2	40.3	0.35	39.74	0.30	40.31	0.31
TiO_2	0.00	0.00	0.01	0.01	0.05	0.04
Al_2O_3	0.09	0.03	0.11	0.07	0.60	0.79
Cr	0.04	0.03	-	-	0.04	0.02
FeO*	7.6	0.43	9.50	0.45	10.55	0.10
MnO	0.09	0.02	0.14	0.01	0.18	0.01
MgO	50.13	0.55	48.85	0.38	47.69	1.11
NiO	0.35	0.05	0.32	0.04	0.22	0.01
CaO	0.31	0.09	0.40	0.03	0.90	0.58
Na_2O	0.01	0.01	0.01	0.01	0.03	0.06
Total	98.92		99.08		100.6	
n	18		16		5	
Fo	92.16	0.47	90.16	0.46	88.96	0.17
E-MORB starting material, 1300°C melting temp.						
SiO_2	40.77	0.37	39.91	0.10	40.4	0.40
TiO_2	0.02	0.01	0.04	0.01	0.02	0.01
Al_2O_3	0.18	0.15	0.09	0.02	0.06	0.04
Cr	0.03	0.02	0.02	0.01	0.02	0.01
FeO*	6.13	0.27	11.38	0.17	10.13	1.32
MnO	0.11	0.02	0.19	0.02	0.15	0.03
MgO	51.33	0.47	47.3	0.18	48.69	1.30
NiO	0.17	0.08	0.25	0.01	0.32	0.05
CaO	0.27	0.07	0.32	0.03	0.22	0.20
Na_2O	0.01	0.01	0.00	0.00	0.01	0.01
Total	99.03		99.51		100.02	
n	15		8		5	
Fo	93.7		89.4		86.7	
HAB starting material, 1300°C melting temp.						
SiO_2			40.07	0.31	40	0.40
TiO_2			0.00	0.01	0.02	0.01
Al_2O_3			0.09	0.03	0.07	0.04
Cr			0.02	0.02	0.03	0.01
FeO*			10.84	0.91	12.23	2.19
MnO			0.16	0.02	0.19	0.05
MgO			48.18	0.77	47.56	1.82
NiO			0.31	0.06	0.31	0.04
CaO			0.25	0.06	0.28	0.15
Na_2O			0.01	0.01	0.02	0.02
Total			99.92		100.55	
n			10		7	
Fo			88.79	0.99	86.93	2.37
	1280° Melt T.		1250° Melt T.		1220° Melt T.	
	Avg	2σ	Avg	2σ	Avg	2σ
Experiment Set 3: Anorthite and Forsterite Saturated Variable Melting Temperatures						
N-MORB starting material, 1210° C equilibration temp.						
SiO_2	39.00	0.24	39.33	0.24	39.34	0.26
TiO_2	0.01	0.01	0.02	0.01	0.02	0.00
Al_2O_3	0.22	0.52	0.07	0.01	0.09	0.01
Cr	0.08	0.02	0.06	0.03	0.10	0.04

Table 5. (continued)

	1280° Melt T.		1250° Melt T.		1220° Melt T.	
	Avg	2σ	Avg	2σ	Avg	2σ
FeO*	10.65	0.39	10.89	0.10	11.13	0.13
MnO	0.17	0.01	0.15	0.01	0.15	0.02
MgO	47.63	0.23	47.73	0.40	46.96	0.43
NiO	0.19	0.05	0.24	0.01	0.19	0.01
CaO	0.45	0.16	0.42	0.01	0.44	0.02
Na_2O	0.01	0.03	0.00	0.00	0.00	0.00
Total	98.41		98.91		99.1	
n	12		3		3	
Fo	87.80	0.32	88.65	0.16	87.79	0.67

spinel observed as inclusions in MORB anorthite megacrysts [*Fisk et al.*, 1982; *Sinton et al.*, 1993], while those produced at 1290° were several wt% more aluminous than natural examples.

[21] Glass compositions, with the exception of CaO, follow a liquid line of descent from the melting temperature of 1300°C through 1210°C with decreasing MgO (Table 3, Figures 7–11). These trends were also colinear, i.e., parallel, to the trends of published data from the source suites of the starting glasses [*Davis and Clague*, 1987; *Karsten et al.*, 1990; *Donnelly-Nolan et al.*, 1991]. Aluminum contents of liquids derived from all three starting glasses fall along a trend from the high-temperature to low-temperature compositions (Figure 7). The increase in the ratio of Al_2O_3 to MgO at higher temperature shows that Al-rich melts were present prior to feldspar crystallization due to the Al component being added through reaction with the capsule during saturation. The Al component decreases with temperature due first to reaction with the capsule through Al-Si cation exchange and the formation of Al-spinel, and then through crystallization of feldspar within the liquid.

[22] For all starting compositions, Na was systematically low (Figure 8). This is possibly due to reaction with the capsule wall, and loss to the furnace atmosphere, although the amount of melt exposed to the atmosphere is small. CaO trends were distinctive for each starting composition and may in part reflect the effects of differing points of the onset of plagioclase crystallization. The CaO

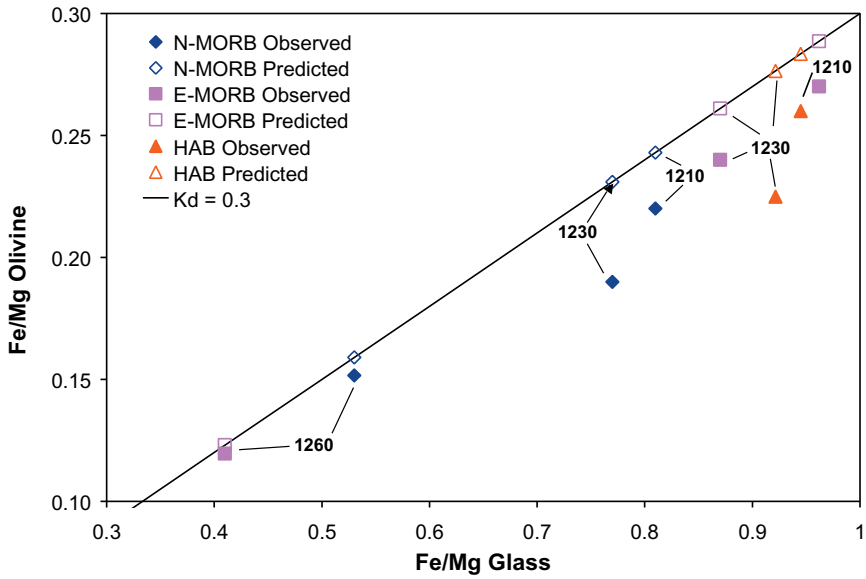

Figure 4. FeO/MgO of olivines that crystallized in the melt versus melt FeO/MgO for Experiment Set 2. Kd line delineates where the points should fall for olivines in equilibrium with melt based on FeO/MgO partition coefficient of 0.3. Labels refer to equilibration temperatures.

content in N-MORB-derived liquids remained nearly constant with decreasing MgO and temperature. The E-MORB-derived melts show a parabolic trend with a minima of 12.15% CaO at 1260° and 11.7% MgO, while the HAB-derived liquids have a less pronounced parabolic trend with the minima of 11.1% CaO at 1230° and 9.31% MgO (Table 3, Figure 9). Although CaO trends do not describe LLDs from the 1300° melt to the starting glass and starting glasses lava suites, the CaO contents of the experiments that nucleated plagioclase (1230° and 1210°) do fall within the range of MORB glass compositions from the RIDGE data set for the Mid-Atlantic Ridge (Figure 9).

[23] The rate of TiO_2 decrease versus increased MgO was enhanced at higher temperature for N-MORB compositions (−0.3 to −0.8 between 1300° and 1290°). E-MORB showed the greatest decrease for each percent increase MgO between 1230° and 1210° C (−0.65), while HAB-derived liquids had a consistent value of a 0.17% decrease in TiO_2 for each percent increase in MgO (Figure 10). The Mg# of the glass remained relatively constant as a function of temperature (~69–80; Table 2), which may represent a buffering effect that was also observed in the linear trends of FeO* versus MgO (Figure 11). The FeO* content of the melts increased with falling temperature and MgO; this trend was linear for N-MORB- and E-MORB-derived melts, while FeO* was relatively constant

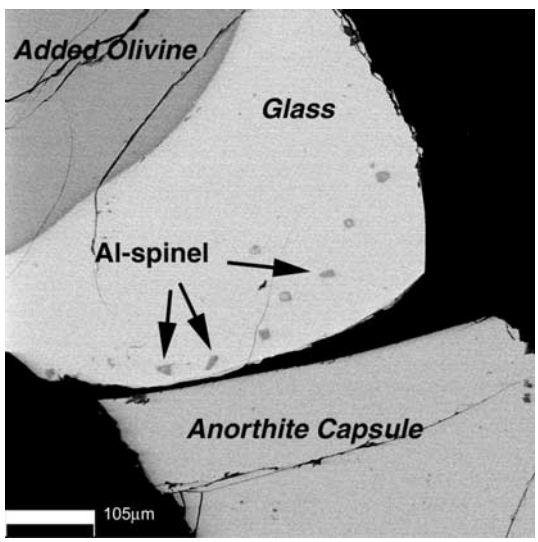

Figure 5. Backscattered electron image of experimental run with an equilibration temperature of 1290° C and equilibration time of 4 hours. Bands of Al-spinel have formed in the melt adjacent to the capsule rim. Anorthite capsule has separated from glass during mounting.

Table 6. Compositions of Spinels Formed in Melt[a]

	N-MORB Starting Material										E-MORB Starting Material		HAB Starting Material			
	1290° Equil. T.[b]		1290° Equil. T.		1260° Equil. T.		1230° Equil. T.		1210° Equil. T.		1290° Equil. T.		1290° Equil. T.		1230° Equil. T.	
	Avg	2σ	Avg	2σ	Avg	2σ	Avg	2σ	Avg	2σ	Avg	2σ	Avg	2σ	Avg	2σ
S_iO_2	0.05	0.12	0.01	0.03	0.08	0.07	0.56	1.22	0.00	0.00	0.00	0.00	0.15	0.07	0.14	0.05
TiO_2	0.03	0.04	0.08	0.02	0.22	0.06	0.26	0.11	0.19	0.01	0.06	0.03	0.04	0.02	0.07	0.02
Al_2O_3	63.50	0.26	61.47	1.90	41.51	4.98	32.95	1.34	31.62	0.39	68.35	0.56	67.21	0.45	67.97	0.26
Cr_2O_3	5.44	0.25	6.03	1.96	28.1	4.45	30.18	0.66	29.37	0.01	0.66	0.52	0.38	0.39	1.34	0.37
FeO*	5.61	0.25	7.46	0.08	10.5	1.68	16.27	2.06	18.73	0.02	4.94	0.22	7.49	0.77	5.81	0.12
Fe^{2+}	4.80	0.27	0.03	0.03	7.38	0.87	9.82	2.46	7.30	0.32	4.17	0.34	0.04	0.03	0.05	0.04
Fe^{3+}	1.07	0.40	7.76	0.08	3.44	0.85	6.77	1.66	14.95	0.02	1.01	0.20	7.83	1.02	5.96	0.13
MnO	0.00	0.00	0.00	0.00	0.04	0.02	0.15	0.02	0.12	0.08	0.00	0.00	0.04	0.02	0.04	0.01
MgO	24.13	0.38	23.98	0.28	20.24	1.01	17.35	0.42	17.19	0.10	25.02	0.32	23.15	0.35	24.62	0.31
ZnO	0.00	0.01	0.03	0.03	0.14	0.14	0.03	0.04	0.05	0.41	0.01	0.02	0.00	0.00	0.00	0.00
V	0.02	0.02	0.04	0.03	0.16	0.06	0.15	0.05	0.12	0.03	0.04	0.03	0.02	0.01	0.05	0.02
Total	99.03		99.43		101.31		98.22		100.91		99.32		98.86		100.24	
n	7		12		5		5		3		10		3		11	
Cr#	0.05	0.03	0.06	0.02	0.31	0.06	0.38	0.01	0.38	0.00	0.01	0.01	0.01	0.00	0.01	0.00
Mg#	0.90	0.01	0.91	0.01	0.83	0.02	0.76	0.05	0.78	0.00	0.91	0.01	0.86	0.01	0.90	0.01
Fe^{3+}#	0.01	0.00	0.01	0.00	0.04	0.01	0.08	0.02	0.08	0.01	0.01	0.00	0.01	0.00	0.01	0.00

[a] Experiment Set 2: Anorthite and Forsterite Saturated.
[b] Experiment with 4 hour run time.

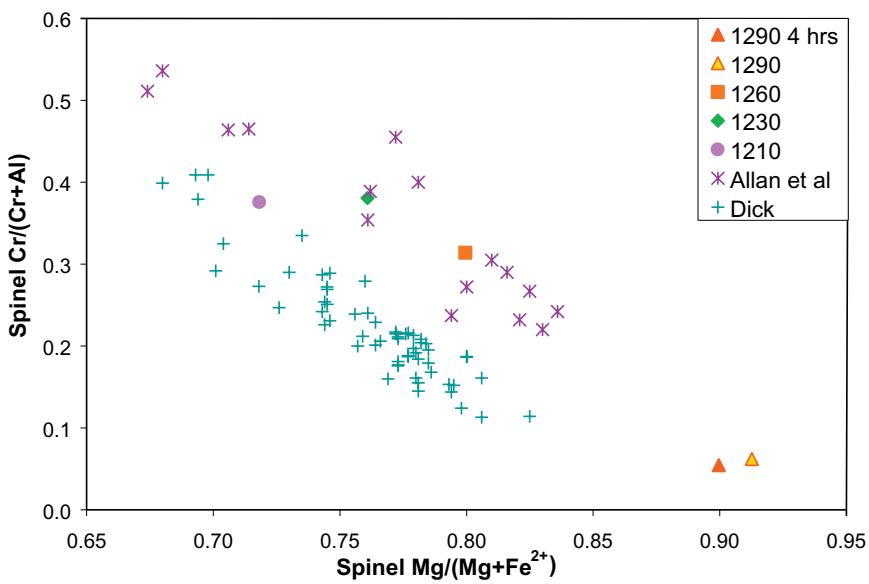

Figure 6. Cr# versus Mg/(Mg + Fe^{2+}) for spinels crystallized from N-MORB-derived liquids in Experiment Set 2. Label numbers refer to equilibration temperature in degrees C. "Dick" refers to the compositions of abyssal peridotite spinels from *Dick* [1989], "Allan et al," refers to compositions of spinels, naturally occurring in lavas of the Lamont Seamount Chain, reported by *Allan et al.* [1989].

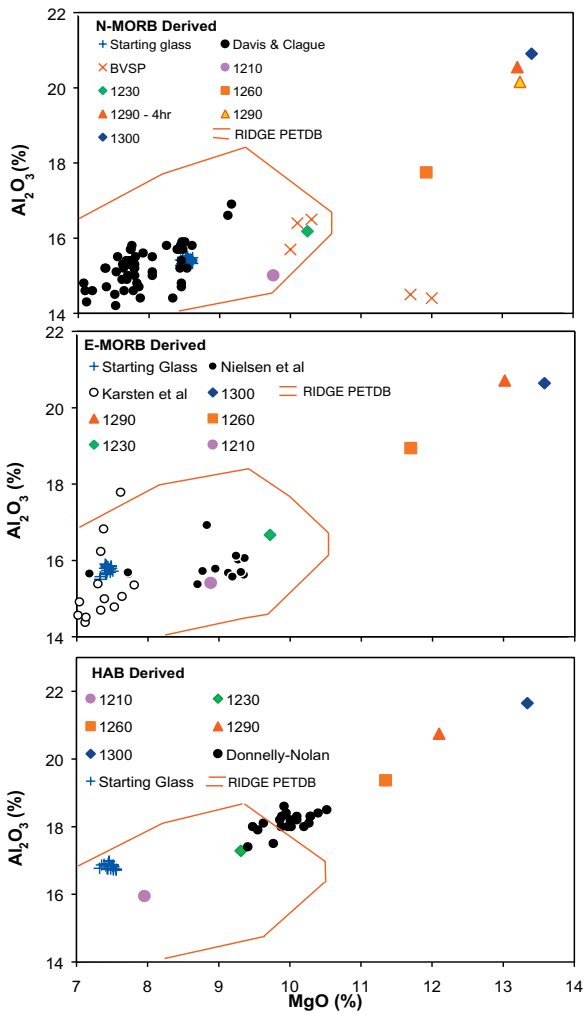

Figure 7. Al_2O_3 versus MgO for Experiment Set 2. Numbers refer to equilibration temperatures. BVSP refers to hypothetical primary MORB magma [*BVSP*, 1981]. Davis and Clague refers to compositions from the Gorda Ridge from *Davis and Clague* [1987]. Karsten et al. refers to Endevour Segment compositions from *Karsten et al.* [1990], Sours-Page et al. refers to melt inclusion compositions from the same segment from *Sours-Page et al.* [1999], Donnelly-Nolan refers to compositions from Giant Crater, Medicine Lake, CA from *Donnelly-Nolan et al.* [1991]. Region outlined in red contains range of Mid-Atlantic Ridge glass compositions in the pre-compiled RIDGE petrologic database (RIDGE PETDB).

between 1230° and 1210° for HAB-derived liquids (Figure 11).

3.3. Experiment Set 3: Anorthite and Forsterite Saturated Melt, Variable Melt T

[24] The third set of experiments separated the effects of equilibration temperature from potential effects of undercooling (ΔT). As described earlier, this was accomplished by keeping the equilibration run temperature fixed at 1210° and varying the initial melting temperatures, which were chosen to repeat the same amounts of undercooling used in experiment set 2.

[25] There was diversity among the compositions of crystallization products. The feldspars from the 70° undercooling experiments had outer rims (~25 μm in the largest crystals) that were An_{81-83} and cores up to An_{96}. With 40° undercooling, the feldspars had thin (~10 μm) An_{91} rims surrounding an An_{94-95} core. Although 10 degrees of undercool-

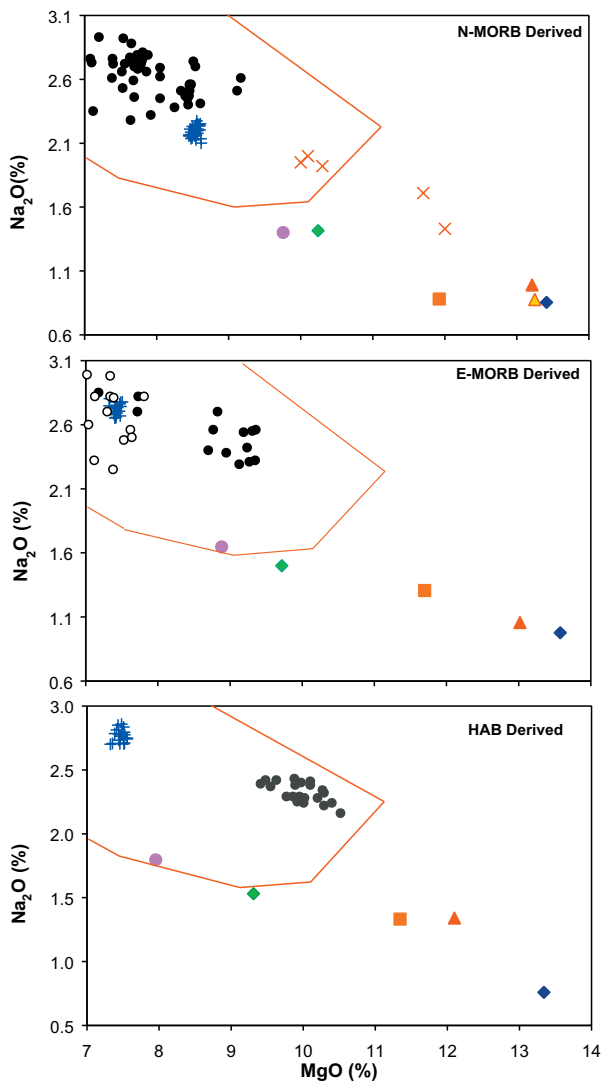

Figure 8. Na_2O versus MgO for Experiment Set 2. Symbols same as Figure 7.

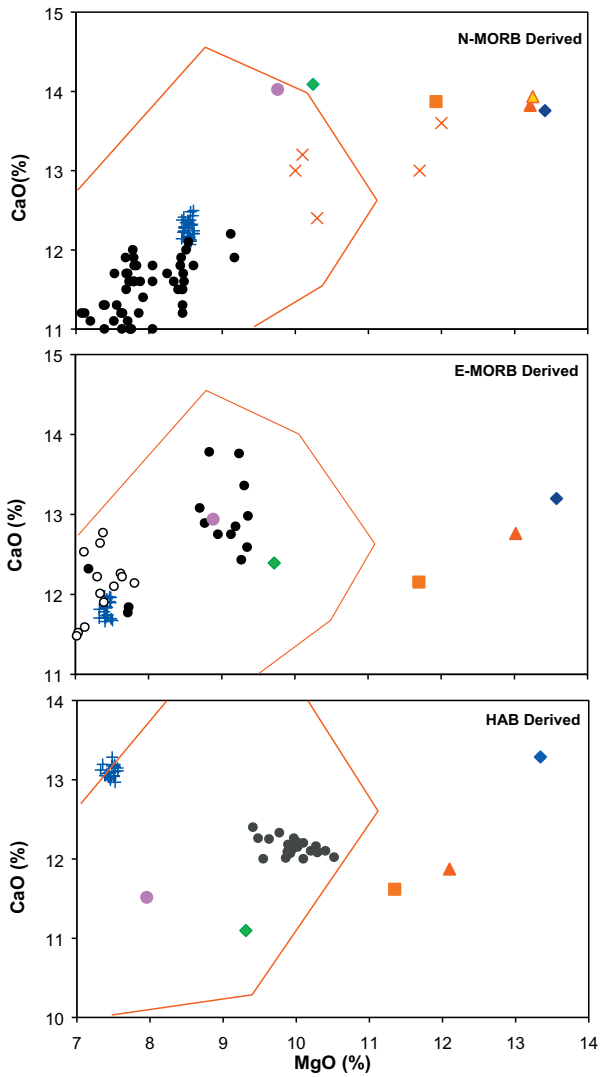

Figure 9. CaO versus MgO for Experiment Set 2. Symbols same as Figure 7.

ing produced the lowest glass Mg# of any forsterite saturated experiment (Table 2), the feldspars produced had the highest average An content of any experiment: $An_{95.5}$. These also had a ~5 μm An_{88} zone on the surface in contact with the melt. Figure 12 shows that moving the melting temperature closer to an equilibration temperature of 1210° (decreasing ΔT) increases difference between the expected and observed An contents of the plagioclase in the melts. This indicates that using an initial melting temperature within the plagioclase crystallization field can produce feldspars that have high-An contents, but are out of equilibrium with the melt. This observation supports our use of a melting temperature of 1300° in Experiment Set 2.

[26] Although there was some diversity among glass compositions from Experiment Set 3, the compositions overall were similar to the 1210° compositions from Experiment Set 2, where the melting temperature was 1300° and ΔT was 90° (Figure 13). There was a systematic variation with MgO content, which decreased as the melting temperature decreased. However, even this variation was minor, from 9.77% with 70 degrees of undercooling (1280°C melting temperature) to 9.38% with 10 degrees undercooling (Table 3). Melt in this experiment

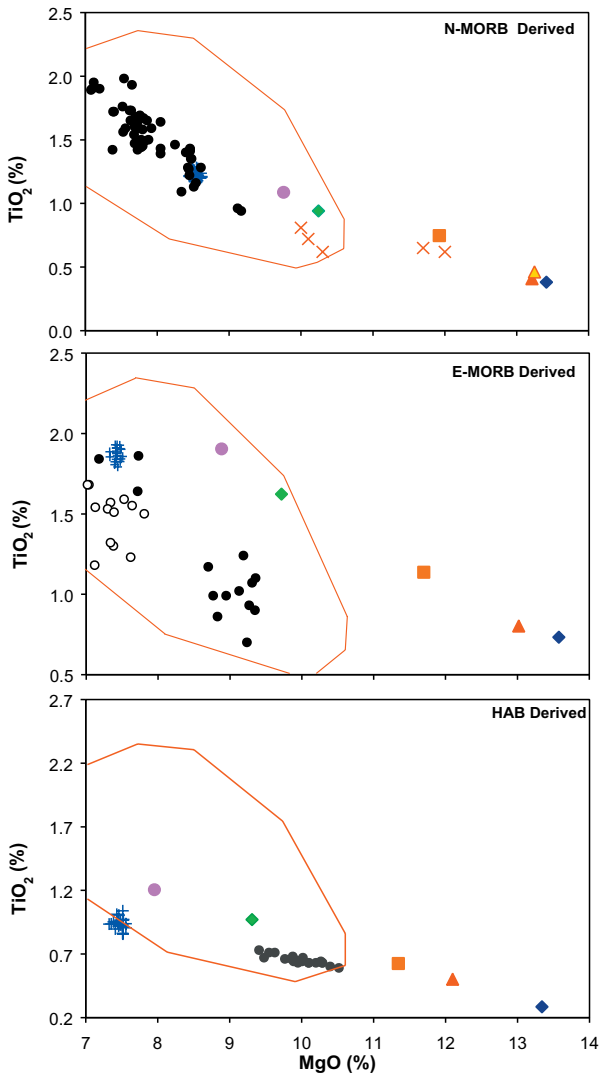

Figure 10. TiO_2 versus MgO for Experiment Set 2. Symbols same as Figure 7.

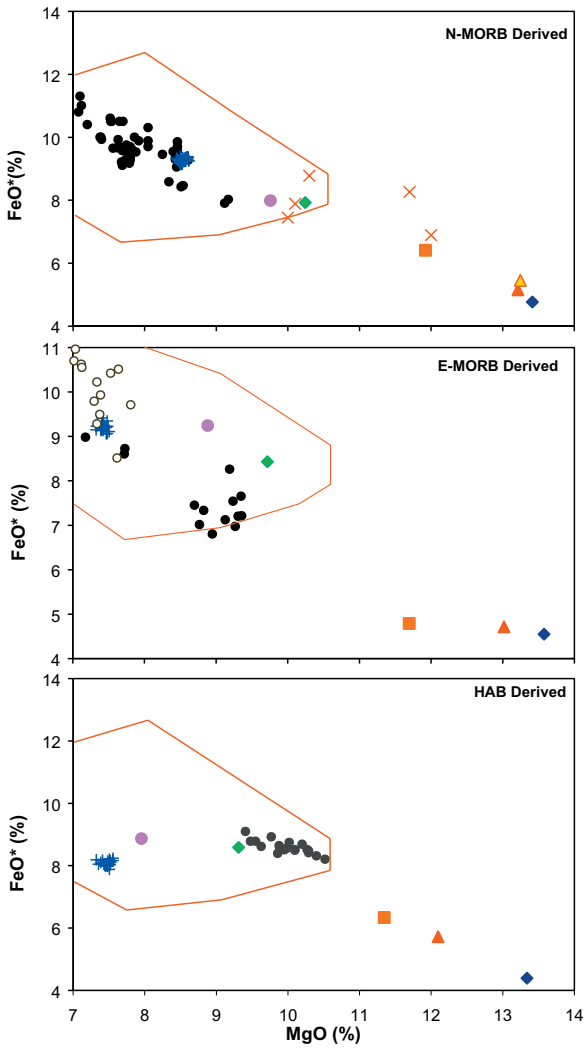

Figure 11. FeO* versus MgO for Experiment Set 2. Symbols same as Figure 7.

also had higher CaO values than other experiments using N-MORB glass, but this was less than 1% compared to other experiments with a 1210° equilibration temperature. Melts with 10 and 40 degrees of undercooling had the lowest glass Mg# (66.9 and 67.4; Table 2).

[27] With 70° of undercooling, euhedral prisms and laths of zoned feldspars were produced. Melt inclusions were common, as were large embayments on the prisms and hollow cores on the laths, with some resorbed faces (Figure 14). The experiment using 40° undercooling crystallized feldspars that were near equant prisms with rounded corners. The feldspars with 10° undercooling had disequilibrium textures, with resorbed faces and corners that resulted in anhedral crystals.

[28] If the trends produced by Experiment Set 3 were over the same range of compositions as Experiment Set 2, then any conclusions we reached about the control equilibration temperature has on composition would be questionable. Instead, the glass compositions from the results of Experiment Set 3 were similar only to the 1210° experiment of set 2. Although decreasing the melting temperature did decrease the MgO content, this variation was minor. This confirms that equilibration temperature has a greater influence on melt composition than the amount of undercooling. However, the disequilibrium textures and zoning of the feldspars indicate that with low melting and saturation temperatures, the 24-hour run time we used was insufficient to achieve feldspar-melt equilibrium. In comparison, when an equilibration temperature of 1290° and a melting temperature of 1300° were used in Experiment Set 2 (which is the same amount of ΔT as the experiment with 1220° melt and 1210° run temperatures), four hours equilibration time was sufficient to produce the same results as 24 hours (Table 3). This indicates that the run temperature is a controlling factor in the speed of equilibration as well.

4. Discussion

[29] The primary goal of these experiments was to determine the composition of anhydrous mafic liquids in equilibrium with high-An feldspar. We must again emphasize that the design of our experimental apparatus should not be mistaken as an attempt to simulate a natural process where primitive melt reacts with plagioclase and we do not intend to propose such a model. Rather, our experiments were designed to saturate melts in anorthitic components at high temperatures, observe the composition of the melts and the phases that crystallize in the melt at lower run temperatures, and compare the results to natural examples. Only then do we propose a model.

[30] In our initial runs (Experiment Set 1), we observed that anorthite saturation alone was not sufficient for producing >An_{85} feldspar or melts that resembled natural lava suites in composition

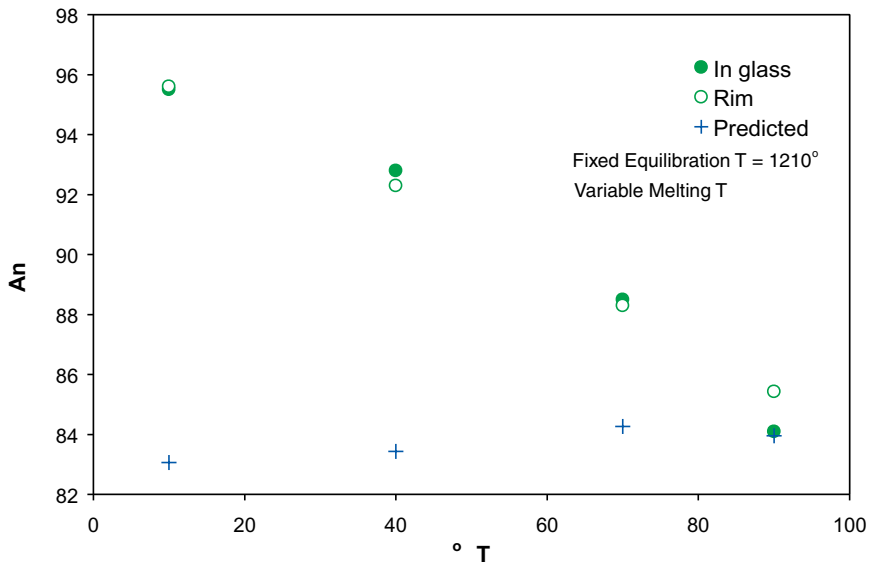

Figure 12. Comparison of observed An values for capsule rim reaction zone (Rim) and feldspar crystallized from the melt (In-glass) to the predicted equilibrium values for variable melting temperatures and ΔT and a fixed equilibration T of 1210°. Note that as the melting T and ΔT decrease, the feldspars are increasing out of equilibrium with the melt. All equilibration times are 24 hours.

(Figures 1 and 2). The experimental liquids did resemble refractory melt inclusions observed by *Johnson et al.* [1995], but these natural examples occurred in feldspars with An > 85.

[31] However, the results of our second set of experiments show that basaltic melt that is in equilibrium with both high-An feldspar and high-Fo olivine is generally similar to natural basalt glasses and melt inclusions hosted by high-anorthite feldspar. The composition of the starting materials (Table 1) may have had some effect in the ability to achieve equilibrium, but it is important to note that the compositions of all liquids once saturated with anorthite and forsterite during the melting period (1300°) were very similar despite the different starting glasses (Tables 1, 2, and 3). The saturated liquids all had high CaO/Na_2O values, and Al# above 30. E-MORB-derived liquids that crystallized plagioclase (i.e., those at 1210° and 1230°) were closest to natural glasses in composition for all major elements, while the olivines that crystallized in E-MORB-derived melts were closest to their predicted equilibrium values (Figure 4). It is possible that the modified HAB and N-MORB compositions would produce better equilibrium results using time-temperature profiles different from those of our experiments. The issues relating to the effects of cooling rate and the length of the equilibration period have been addressed in another group of experiments that also dealt with melt inclusion formation [*Nielsen and Kohut*, 2000; *Kohut and Nielsen*, 2002] and will be reported in full in a separate paper (E. J. Kohut and R. L. Nielsen, Melt inclusion formation mechanisms and compositional effects in high-An feldspar and high-Fo olivine in anhydrous mafic silicate liquids, submitted to *Contributions to Mineralogy and Petrology*, 2003).

[32] The similarity of the compositions our glasses that crystallized high-An feldspar from experiment sets 2 and 3 to the relevant starting glasses [*Karsten et al.*, 1990; *Donnelly-Nolan et al.*, 1991; *Davis and Clague*, 1987] and natural basalt arrays (RIDGE PETDB), is an important difference between our experiments and those of *Panjasawatwong et al.* [1995]. While they also produced liquids in equilibrium with high-An feldspar, their glass compositions did not resemble natural basalt suites and due to their lower MgO contents do not fall within the limits of the data we present on Figures 7–11. However, while *Panjasawatwong et al.* [1995] did raise the Al content and Ca/Na ratio

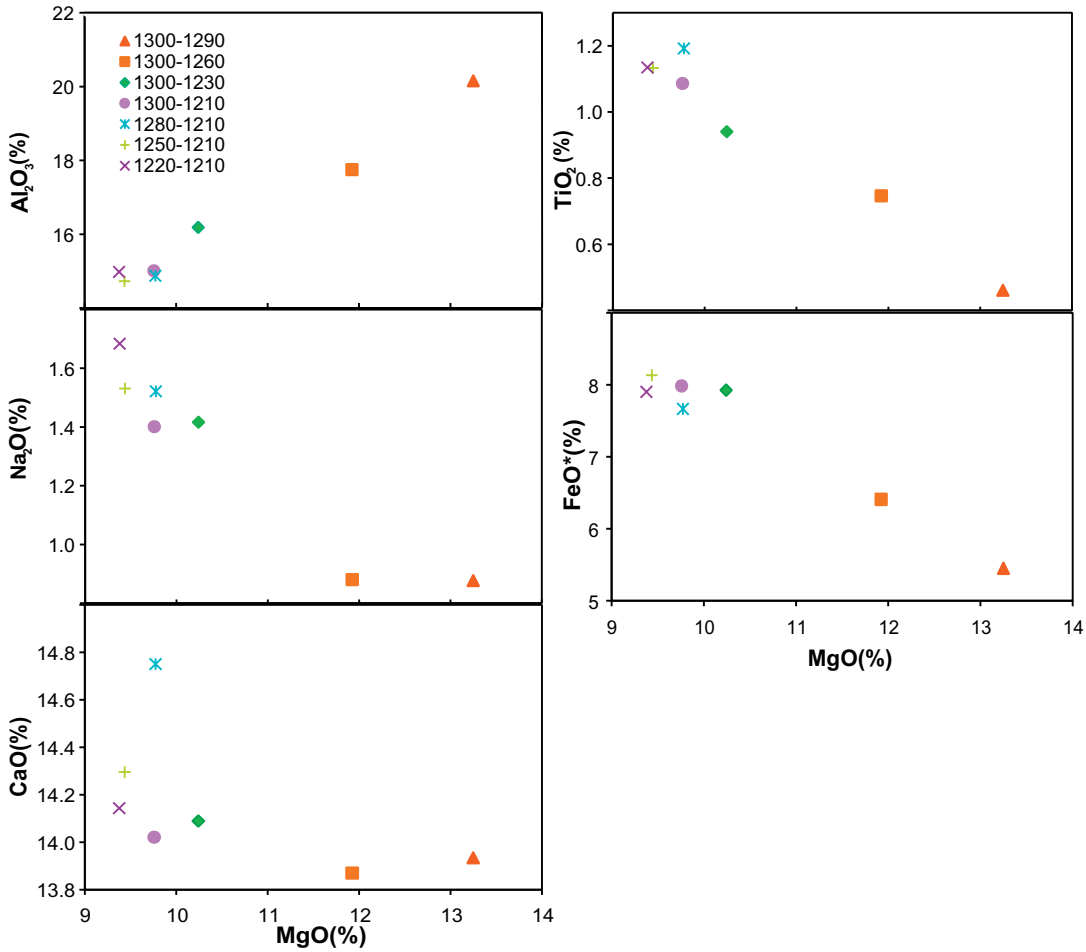

Figure 13. Comparison of the compositions of melts from Experiment Set 2 to Experiment Set 3. First number refers to melting temperature, second to equilibration run temperature. Set 2 experiments have 1300° melt T. Note that compositions from Set 3 are similar to the 1210° experiment from Set 2, showing that equilibration T has a greater influence on melt compositions than melt T or ΔT.

of their melts, they did not saturate their liquids with forsterite. We observed that the melt saturated in forsterite as well as anorthite at high temperature when cooled produced $An_{81.5-87}$ feldspar in equilibrium with the melt; as noted earlier, the initial experiments saturated in only anorthite crystallized An_{76-79} feldspars. The additional phase, high-Fo olivine, may limit the degrees of freedom in the system and constrain the phases to those on the forsterite-anorthite cotectic, which would favor plagioclase with a high-An content (Figure 15). It is significant that the liquids are constrained to this cotectic, as high-An and high-Fo olivine are the first crystallizing phases in most primitive MORB lavas [*Sinton et al.*, 1993; *Nielsen et al.*, 1995]. However, no liquids with such high Mg# that follow this cotectic have been produced experimentally prior to now. In addition, the host glass MgO and plagioclase An contents of Experiment Set 2 are similar to feldspar An content and melt inclusion compositions described by *Sours-Page et al.* [1999, 2002]. These similarities to natural systems suggest that our experiments are valid analogs for some magmas parental to anorthite-bearing anhydrous basalts.

[33] The mineralogy and composition of experimental run products at 1230° and 1210° are also similar to primitive lavas of the Sasha Seamount of the Lamont Seamounts. The significance of this is that the Lamont Seamounts occur off-axis and the similarity to our compositions indicates that

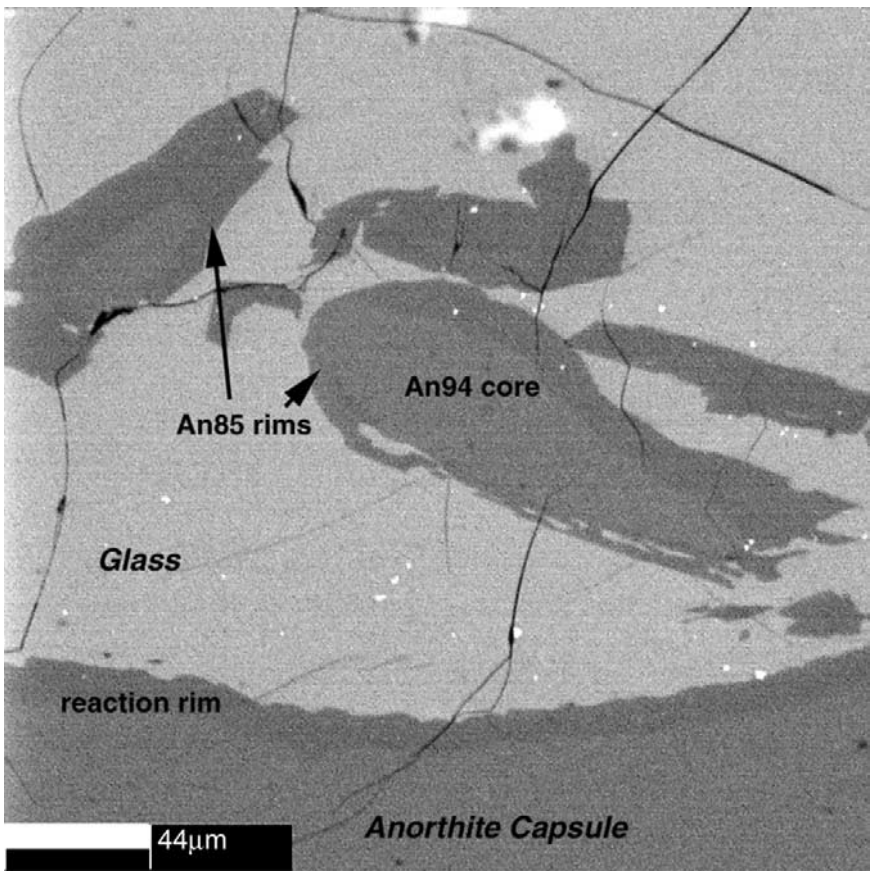

Figure 14. Backscattered electron image of run products of experiment with a melting temperature of 1280° and equilibration temperature of 1210° (ΔT = 70°). Dark gray is feldspar, light gray is quenched melt. Note zoning of the feldspars and disequilibrium texture of some faces on the crystals.

the experiments are also applicable to anhydrous melts that do not originate at mid-ocean spreading centers. The Sasha Seamount lavas have MgO contents up to 9.7%, Mg# up to 72, and contain Fo_{85-91} olivine, An_{70-91} plagioclase phenocrysts and Cr-rich spinel [*Allan et al.*, 1989]. The calculated normative phase relations of the most primitive Lamont Seamount lavas were reported by *Allan et al.* [1989] to be consistent with formation at shallow pressures (below 10 kb) and at temperatures of 1200°–1240° C. These suggested conditions of formation correlate well with our experimental parameters.

[34] The observation of Al-spinel at 1290°, (anorthite/forsterite saturated experiments) despite no spinel having been added to the starting mixtures indicates that liquids that are in equilibrium with anorthite and forsterite at lower temperatures are in

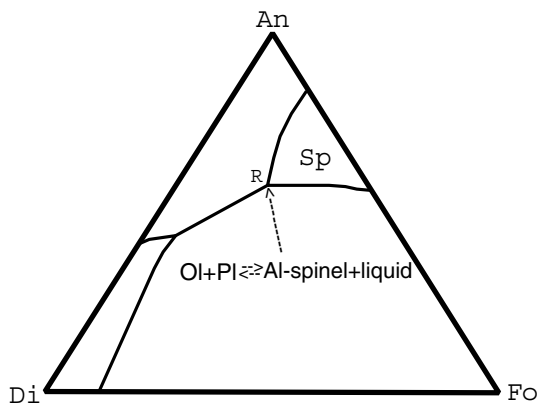

Figure 15. atm An-Fo-Di ternary with spinel field (modified from *Osborn and Tait* [1952]). Aluminous spinel reacting with liquid at reaction point R produces highAn plagioclase and highFo olivine. Crystallization then proceeds along the olivineplagioclase cotectic.

equilibrium with Al-spinel at this temperature. This is what the An-Fo-Di ternary diagram (Figure 15) would predict, and we suggest that our 1290° experiments fall within the spinel field of the ternary. As the run temperatures decrease, our experiments progress along the olivine-plagioclase cotectic of the ternary diagram with decreasing temperature. To reach the olivine-plagiclase cotectic, the liquid composition must pass first through point R (Figure 15), where Al-spinel will react with the remaining liquid to produce high-An plagioclase and high-Fo olivine. For our experiments, a ternary diagram with a larger spinel field may be appropriate, as the starting compositions contain small amounts of Cr (Table 3). Trace amounts of Cr will stabilize a larger Al-spinel field in ternary space at the expense of anorthite, and can move the reaction point to a lower temperature, e.g., ~1275°C [*Onuma and Tohara*, 1983]. The An-Fo-Di ternary diagram of *Osborn and Tait* [1952], upon which Figure 15 is based, has the reaction point at a higher temperature (~1320°) than those used in our experiments.

[35] The compositions of spinel and olivine in the run products are similar to those in natural, primitive mafic lavas. The compositions of olivines that crystallized in the liquids at run temperatures of 1260° (Table 2) demonstrate that our experiments were in equilibrium with high-Fo olivine, similar to mantle olivine [*Dick and Fisher*, 1983]. The spinel compositions are a function of experimental temperature, with Al content decreasing and Cr/Al content increasing, with decreasing temperature (Figure 6). While, the high-Al spinels formed in bands, the chromites at lower temperatures in the N-MORB experiments formed throughout the liquid. This provides evidence that the liquid assimilates the Al-spinel with decreasing temperature, and the lack of Al-spinel at lower temperatures indicates that the system has proceeded past the reaction point. The Al-spinel observed at 1230° for the HAB-derived melts may indicate that particular system is still at the reaction point at lower temperatures, or it may indicate that with the HAB starting composition, our time-temperature profile was not suitable for achieving true equilibrium results at 1230° run temperature and 70° ΔT.

[36] One possible mechanism for producing the observed compositional trends is to buffer an evolving magma with Al-spinel, similar to those characteristic of the most primitive MORB and depleted seamount lavas and some abyssal peridotites [*Dick and Bullen*, 1984; *Allan et al.*, 1989]. The reaction of a primitive magma with the spinel would maintain high Al_2O_3 and MgO contents at the reaction point (R in Figure 15), where the melt is three-phase (anorthite-fosterite-spinel) saturated. As the Al-spinel is consumed, the reaction proceeds along the fosterite-anorthite cotectic (Figure 15). This would result in the reaction Al-sp + liquid → pl + ol ± chromite with decreasing temperature.

[37] The third set of experiments illustrate that while moving the initial melting temperature close to the equilibration run temperature does not greatly effect the liquid composition, it does effect the chemistry of the crystallizing feldspars, and these are further from equilibrium with the melts as ΔT decreases (Figure 12). This indicates that the smaller the difference between the melt and equilibration temperature, the greater the amount of time required to achieve equilibrium. We suggest that the feldspars that formed early during the equilibration period may have had higher-An values and were out of equilibrium with the host liquid. As the equilibration period progresses, rims form on the early formed feldspars that have An contents closer to equilibrium with the melt and eventually the entire feldspar would equilibrate with the melt. Later formed feldspars would be in equilibrium with the melt. The length of the required equilibration period though, depends on both undercooling and the temperature of equilibration; the experiment with an equilibration temperature of 1230° from Set 2 also had a ΔT of 70°, yet the feldspars were in equilibrium with the melt. This indicates that while at any run temperature decreasing ΔT may require an increase in the length of the time required to achieve melt/crystallizing mineral equilibrium, this effect becomes more pronounced at lower equilibration temperatures. With regards to the Al-spinel/liquid reaction just described, we suggest that the lower the temperature of the liquid reacting with the spinel, the longer the period of time needed for the liquid to react.

Table 7. Crystallization as a Function MgO and Temperature Based on Change in TiO_2

T Change	N-MORB	E-MORB	HAB
% Crystallization Based on TiO_2Change			
1300-1290	7.32	8.75	44.00
1300–1260	49.33	35.96	55.56
1300–1230	59.57	54.94	71.13
1300–1210	63.11	61.58	76.86
T Change	N-MORB	E-MORB	HAB
% Crystallization per MgO% Decrease			
1300–1290	36.59	15.63	35.48
1300–1260	32.89	19.13	27.92
1300–1230	18.79	14.23	17.65
1300–1210	17.34	14.34	14.39
Average	26.4	15.83	23.86

[38] The amount of crystallization in our experiments as a function of temperature was estimated using the trend of TiO_2 versus MgO. For systems saturated with Al-spinel, plagioclase and olivine, Ti can be considered an almost completely incompatible element (D = 0). For any completely incompatible element, the Rayleigh distillation equation simplifies to $F \cong C_o^l/C^l$ (where F is the amount of liquid remaining, and C_o^l and C^l are the initial and current concentration of the trace element in the liquid respectively). If one then assumes a bulk D_{Ti} of 0 for this assemblage, the Ti content in the glass will vary only by the ratio of the liquid/solid fraction. Using the TiO_2 content correlated with MgO, we can calculate the percent crystallization for each percent decrease in MgO and correlate that with the temperature in our experiments.

[39] The results of our calculations (Table 7) indicate large amounts of crystallization would occur for each percent decrease in MgO: these average ~27% for N-MORB-derived, ~16% for E-MORB-derived, and ~24% for HAB-derived melts. However, these averages cannot be extrapolated linearly, as the HAB- and N-MORB-derived liquids had higher calculated rates of crystallization per % decrease MgO at 1260° and 1290° (28–35% and 35–37% respectively) than at 1230° and 1210° (Figure 16). If our 1230° and 1210° experiments are valid analogs of natural primitive basalts (≥8% MgO), then even primitive MORB lavas may have undergone a large amount, 62–77%, of crystallization prior to eruption (Table 7). These amounts however, must be examined in the context of the buffering effect the added olivine crystal and anorthite capsule.

[40] We attempted to produce numerical models for our data using the MELTS [*Ghiorso and Sack*, 1995] and MIXNFRAC [*Nielsen*, 1990] algorithms. Although neither program was able to produce a model that accurately reflected our

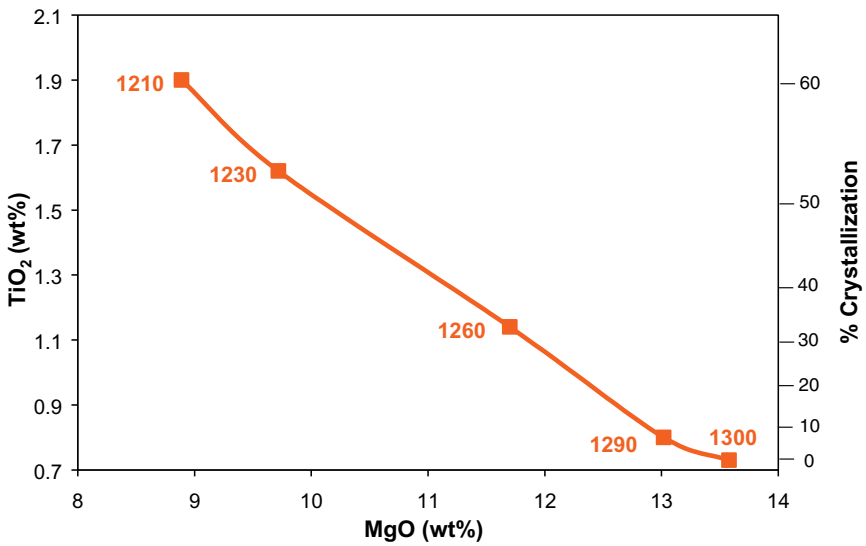

Figure 16. TiO_2 content and % crystallization as functions of MgO content of experiments using EMORB starting compositions. Labels of points in plot refer to equilibration temperature.

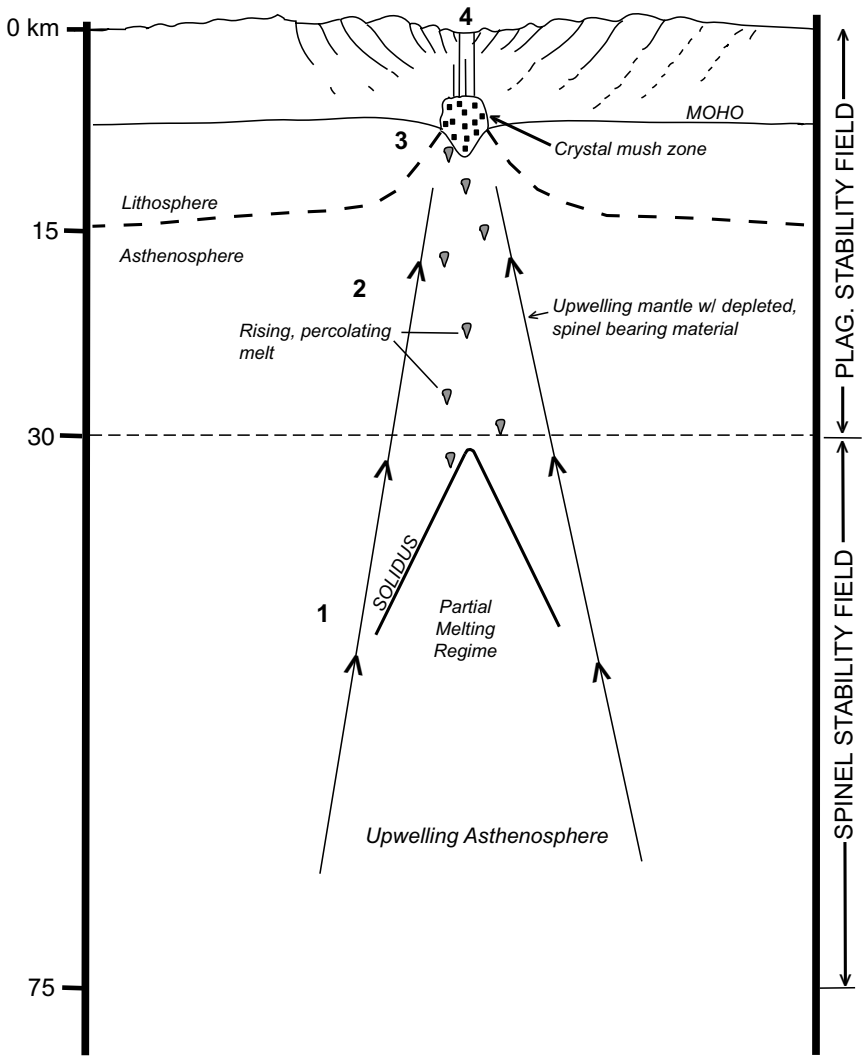

Figure 17. Possible scenario for the petrogenesis of anorthitebearing MORB. 1) Mantle upwelling leads to partial melting of lherzolite, producing a primitive melt. 2) Rising melts percolate through upper mantle, including spinelbearing residual mantle that is displaced into plagioclase stability field by upwelling. Melt reacts with Alspinel and is driven toward plagioclase saturation. This can occur anywhere below the base of the crust, including fracture channels in harzburgite 3) Melt (now Alrich due to reaction with spinel) accumulates prior to eruption in crystal mush zone/conduit system below ridge. HighAn phenocrysts form as crystallization proceeds along anorthite/fosterite cotectic. 4) Anorthitebearing MORB is erupted.

results, the assimilation model provided trends that were similar to the experimental data. The predicted phase assemblages also concurred with our lack of pyroxene saturation in the experiments. Nevertheless, the results were even more illustrative of our need to recalibrate our models to these melt compositions. Currently, we are clearly not in a position where we can adequately simulate magmatic processes for this abundant, very primitive precursor class of basaltic magmas.

[41] While we do not discount the fact that anorthite in MORB can originate from the primary melting of refractory material [*Natland*, 1989; *Johnson et al.*, 1995], we propose that our results indicate that other mechanisms for producing high–An feldspar may also exist that explain other, more recent melt inclusion data [e.g., *Sours-Page et al.*, 2002]. We suggest that the evidence outlined above is consistent with a model wherein anorthite in MORB may result from primitive, olivine saturated melt reacting with spinel in depleted material

in the uppermost mantle prior to transport into the crustal magma system. As conceived here, this would take place above the melting regime, but below the crust (Figure 17) and would therefore not require primary melting of refractory material at depth. Percolation of magma through this spinel-bearing upper mantle (displaced into the plagioclase stability field in the upwelling asthenosphere) would result in the melt being driven to plagioclase saturation and away from pyroxene saturation (addition of Al, buffered Mg, Ca). Melt could react with spinel-bearing depleted material anywhere in the asthenospheric diapir, and could also react with spinel as it moved through fractures in harzburgite at the base of the crust. This process is similar to the one described by *Dick and Natland* [1996] for the origin of high alumina and calcic melts capable of producing the An_{99} feldspars they observed in gabbros ODP Site 895. The major difference was that high-magnesium diopside is also present in the gabbroic segregations they examined, which indicates that those magmas were driven toward pyroxene saturation. Nonetheless, their observations do provide field evidence of a melt reaction at low pressure capable of producing melts that will crystallize high-An feldspar. We suggest that our hypothesis can be tested experimentally. Such experiments could be designed to react primitive liquids with Al-spinel over a range of temperatures, pressures and time. In this way the role of primary refractory melts versus reaction with refractory spinel in anorthite-bearing anhydrous basalts can be examined.

5. Conclusions

[42] The results of our experiments indicate that it is possible to experimentally produce anorthite and Fo_{90} saturated primitive basaltic liquids close in composition to naturally occurring lavas. The experimental liquids are also saturated with Al-rich spinel that is similar in composition to spinels observed in naturally occurring anorthite megacrysts [*Fisk et al.*, 1982; *Allan et al.*, 1989; *Dick*, 1989; *Sinton et al.*, 1993]. This association suggests the possibility that primitive MORB basalts are high-An plagioclase saturated due to continued reaction with the upper mantle above the melting regime. Such a reaction of the rising basaltic magma with the spinel in the depleted upper mantle at depths less than 10 kb would drive the magma toward saturation with feldspar. In essence, high-An feldspar in MORB may be produced by a buffering reaction at the Sp + liquid → Fo + An reaction point. Our experiments also indicate that this buffering reaction will result in an average of ~16–26 % crystallization for each percent decrease in MgO. These data suggest primitive MORB lavas (>8% MgO) have undergone ~62–77% fractionation and reaction with the uppermost mantle and lower crust before eruption.

Acknowledgments

[43] We wish to thank the reviewers and editors for the helpful critique and suggestions, especially J. Maclennan for his suggestions on performing equilibrium comparisons and J. Natland for his emphasis on the wealth of ODP data. Phase equilibria experiments funded by NSF grant EAR 9903137.

References

Allan, J. F., R. Batiza, M. R. Perfit, D. J. Fornari, and R. O. Sack, Petrology of lavas from the Lamont seamount chain and adjacent East Pacific Rise, 10°N, *J. Petrol.*, *30*, 1245–1298, 1989.

Baker, M. B., T. L. Grove, R. J. Kinzler, J. M. Donnelly-Nolan, and G. A. Wandless, Origin of compositional zonation (high alumina basaltic andesite) in the Giant Crater Lava Field, Medicine Lake Volcano, northern California, *J. Geophys. Res.*, *96*, 21,819–21,842, 1991.

Basaltic Volcanism Study Project (BVSP), Ocean-floor basaltic volcanism, in *Basaltic Volcanism on the Terrestrial Planets*, pp. 132–160, Pergamon, New York, 1981.

Cervantes, P., and P. Wallace, Water in subduction zone magmatism: New insight from melt inclusions in high-Mg basalts from central Mexico, *Eos Trans. AGU*, *81*(48), Fall Meet. Suppl., abstract V21G-03, 2000.

Danyushevsky, L. V., M. R. Carroll, and T. J. Falloon, Origin of high-An plagioclase in Tongan high-ca boninites: Implications for plagioclase-melt equilibria at low (PH_2O), *Can. Mineral.*, *35*, 313–326, 1997.

Davis, A. S., and D. A. Clague, Geochemistry, mineralogy, and petrogenesis of basalt from the Gorda Ridge, *J. Geophys. Res.*, *92*, 10,467–10,483, 1987.

Dick, H. J. B., Abyssal peridotites, very slow spreading ridges and ocean ridge magmatism, in *Magmatism in the Ocean Basins*, edited by A. D. Saunders and M. J. Norry, *Geol. Soc. Spec. Publ.*, *42*, 71–106, 1989.

Dick, H. J. B., and T. Bullen, Chromian spinel as a petrogenetic indicator in abyssal and alpine-type peridotites and spatially associated lavas, *Contrib. Mineral. Petrol.*, *86*, 54–76, 1984.

Dick, H. J. B., and R. L. Fisher, Mineralogic studies of the residues of mantle melting: Abyssal and alpine type peridotites, in *Kimberlites II: The Mantle and Crust-Mantle Relationships*, edited by J. Kornprobst, pp. 295–308, Elsevier Sci., New York, 1983.

Dick, H. J. B., and J. H. Natland, Late-stage melt evolution and transport in the shallow mantle beneath the East Pacific Rise, *Proc. Ocean Drill. Program Sci. Results*, *147*, 103–134, 1996.

Donnelly-Nolan, J. M., D. E. Champion, T. L. Grove, M. B. Baker, J. E. Taggert, and P. E. Bruggman, The Giant Crater Lava Field, Geology and geochemistry of a compositionally zoned, high alumina basalt to basaltic andesite eruption at Medicine Lake Volcano, *J. Geophys. Res.*, *96*, 21,843–21,863, 1991.

Dungan, M. A., and J. M. Rhodes, Residual glasses and melt inclusions in basalts form DSDP Legs 45 and 46: Evidence for magma mixing, *Contrib. Mineral. Petrol.*, *67*, 417–431, 1978.

Elthon, D., Pressure of origin of primary mid-ocean ridge basalts, in *Magmatism in the Ocean Basins*, edited by A. D. Saunders and M. J. Norry, *Geol. Soc. Spec. Publ.*, *42*, 125–136, 1989.

Fisk, M. R., Depths and temperatures of mid-ocean-ridge magma chambers and the composition of their source magmas, in *Ophiolites and Oceanic Lithosphere*, edited by I. G. Gass, S. J. Lippard, and A. W. Shelton, *Geol. Soc. Spec. Publ.*, *13*, 17–32, 1984.

Fisk, M. R., A. E. Bence, and J. G. Schilling, Major element geochemistry of Galapagos Rift Zone magmas and their phenocrysts, *Earth. Planet. Sci. Lett.*, *61*, 171–189, 1982.

Fram, M. S., and J. Longhi, Phase equilibria of dikes associated with Proterozoic anorthite complexes, *Am. Mineral.*, *77*, 117–136, 1992.

Gaetani, G. A., and E. B. Watson, Open system behavior of olivine-hosted melt inclusions, *Earth Planet. Sci. Lett.*, *183*, 27–41, 2000.

Ghiorso, M. S., and R. O. Sack, Chemical mass transfer of in magmatic processes; IV, A revised and internally consistent thermodynamic model for the interpolation and extrapolation of liquid-solid equilibria in magmatic systems at elevated temperatures and pressures, *Contrib. Mineral. Petrol.*, *119*, 197–212, 1995.

Grove, T. L., M. B. Baker, and R. J. Kinzler, Coupled CaAl-NaSi diffusion in plagioclase feldspar: Experiments and application to cooling rate speedometry, *Geochim. Cosmochim. Acta*, *48*, 2113–2121, 1984.

Johnson, K. T. M., M. R. Fisk, and H. R. Naslund, Geochemical characteristics of refractory silicate melt inclusions from Leg 140 diabases, *Proc. Ocean Drill. Program Sci. Results*, *137/140*, 131–139, 1995.

Karsten, J. L., J. R. Delaney, J. M. Rhodes, and R. A. Liias, Spatial and temporal evolution of magmatic systems beneath the Endeavor Segment, Juan de Fuca Ridge: Tectonic and petrologic constraints, *J. Geophys. Res.*, *95*, 19,235–19,256, 1990.

Kohut, E. J., and R. L. Nielsen, Cooling rate and isothermal crystallization effects on melt inclusion formation in MORB high-An feldspar and high-Fo olivine, *Eos Trans. AGU*, *83*(47), Fall Meet Suppl., abstract V22A-1213, 2002.

Korenga, J., and P. B. Kelemen, Origin of gabbro sills in the Moho transition zone of the Oman ophiolite: Implications for magma transport in the lower crust, *J. Geophys. Res.*, *102*, 27,729–27,749, 1997.

Maclennan, J., D. McKenzie, K. Gronvold, and L. Slater, Crustal accretion under northern Iceland, *Earth Planet. Sci. Lett.*, *191*, 295–310, 2001.

Marsh, B. D., J. Fournelle, J. D. Myers, and C. I. M. hou, On plagioclase thermometry in island arc rocks: Experiments and theory, in *Fluid-Mineral Interactions: A Tribute to H. P. Eugster*, edited by R. J. Spencer and I.-M. Chou, *Geol. Soc. Spec. Publ.*, *2*, 65–83, 1990.

Muir, I. D., and C. E. Tilley, Basalts from the northern part of the rift zone of the Mid-Atlantic Ridge, *J. Petrol.*, *5*, 409–434, 1964.

Natland, J. H., Partial melting of a lithologically heterogeneous mantle: Inferences from crystallization histories of magnesian abyssal tholeittes from the Siquerios Fracture Zone, in *Magmatism in the Ocean Basins*, edited by A. D. Saunders and M. J. Norry, *Geol. Soc. Spec. Publ.*, *42*, 41–70, 1989.

Natland, J. H., A. C. Adamson, C. Laverne, W. G. Melson, and T. O'Hearn, A compositionally nearly steady-state magma chamber at the Costa Rica Rift: Evidence from basalt glass and mineral data DSDP Sites 501, 504, and 505, *Initial Rep. Deep Sea Drill. Proj.*, *69*, 1065–1077, 1983.

Nielsen, R. L., Simulation of igneous differentiation processes, in *Modern Methods of Igneous Petrology, Rev. Mineral.*, vol. 24, edited by J. Nicholls and J. K. Russel, pp. 65–106, Mineral. Soc. of Am., Washington, D. C., 1990.

Nielsen, R. L., and E. J. Kohut, Melt inclusion formation mechanisms in MORB high-An feldspar, *Eos Trans. AGU*, *81*(48), Fall Meet. Suppl., abstract V51A-10, 2000.

Nielsen, R. L., J. Crum, R. Bourgeois, K. Hascall, L. M. Forsythe, M. R. Fisk, and D. M. Christie, Melt inclusions in high-An plagioclase from the Gorda Ridge, an example of the local diversity of MORB parent magmas, *Contrib. Mineral. Petrol.*, v. *122*, 34–50, 1995.

Nye, C. J., and M. R. Reid, Geochemistry of primary and least fractionated lavas from Okmok volcano, central Aleutians: Implications for arc magmagenesis, *J. Geophys. Res.*, *91*, 10,271–10,287, 1986.

Onuma, K., and T. Tohara, Effect of chromium on phase relations in the join forsterite-anorthite-diopside in air at 1 atm, *Contrib. Mineral. Petrol.*, *84*, 174–181, 1983.

Osborn, E. F., and D. B. Tait, The system diopside-anorthite-forsterite, *Am. J. Sci.*, Bowen Volume, pp. 413–433, 1952.

Panjasawatwong, Y., L. V. Danysushevsky, A. J. Crawford, and K. L. Harris, An experimental study of the effects of melt composition on plagioclase-melt equilibria at 5 and 10 kbar: Implications for the origin of high An plagioclase in arc and MORB magmas, *Contrib. Mineral. Petrol.*, *18*, 420–435, 1995.

Ribbe, P. H., Aluminum-silicon order in feldspars: Domain textures and diffraction patterns, in *Feldspar Mineralogy, Rev. Mineral.*, vol. 2, 2nd ed., edited by P. H. Ribbe, pp. 21–54, Mineral. Soc. of Am., Washington, D. C., 1983.

Roeder, P. L., and R. F. Emslie, Olivine-liquid equilibrium, *Contrib. Mineral. Petrol.*, *29*, 275–289, 1970.

Sinton, C. W., D. M. Christie, V. L. Coombs, R. L. Nielsen, and M. R. Fisk, Near-primary melt inclusions in anorthite phenocrysts from the Galapagos Platform, *Earth Planet. Sci. Lett.*, *119*, 527–537, 1993.

Sisson, T. W., and S. Bronto, Evidence for pressure-release melting beneath magmatic arcs from basalt at Galunggung, Indonesia, *Nature*, *391*, 883–886, 1998.

Sisson, T. W., and T. L. Grove, Experimental investigations of the role of H_2O in calc-alkaline differentiation and subduction zone magmatism, *Contrib. Mineral. Petrol.*, *113*, 143–166, 1993.

Sours-Page, R., K. T. M. Johnson, R. L. Nielsen, and J. L. Karsten, Local and regional variation of MORB parent magmas: Evidence from melt inclusions from the Endeavour segment of the Juan de Fuca Ridge, *Contrib. Mineral. Petrol.*, *134*, 342–363, 1999.

Sours-Page, R., R. L. Nielsen, and R. Batiza, Melt inclusions as indicators of parental magma diversity on the northern East Pacific Rise, *Chem. Geol.*, *183*, 237–261, 2002.